

AD-757 879

SELECTION OF OPTIMAL STABILITY AUGMENTATION SYSTEM PARAMETERS FOR A HIGH PERFORMANCE AIRCRAFT USING PITCH PAPER PILOT

Robert P. Denaro, et al

Air Force Institute of Technology
Wright-Patterson Air Force Base, Ohio

17 October 1972

DISTRIBUTED BY:

NTIS

National Technical Information Service
U. S. DEPARTMENT OF COMMERCE
5285 Port Royal Road, Springfield Va. 22151

AD 757879



Reproduced by
NATIONAL TECHNICAL
INFORMATION SERVICE
U.S. Department of Commerce
Springfield, VA 22151

UNITED STATES AIR FORCE
AIR UNIVERSITY

AIR FORCE INSTITUTE OF TECHNOLOGY

Wright-Patterson Air Force Base, Ohio

D D C
RECEIVED
APR 78 1973
E

113

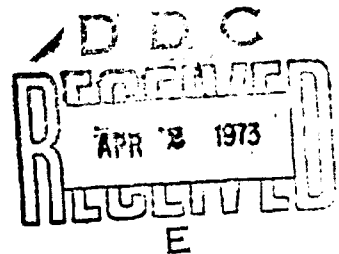
Selection of Optimal Stability
Augmentation System Parameters
For a High Performance Aircraft
Using Pitch Paper Pilot

THESIS

Robert P. Denaro
Lieutenant USAF

GGC/EE/73-3

Garrison L. Greenleaf
Lieutenant USAF



This document has been approved for public
release and sale; its distribution is unlimited.

SELECTION OF
OPTIMAL STABILITY AUGMENTATION SYSTEM PARAMETERS .
FOR A HIGH PERFORMANCE AIRCRAFT
USING PITCH PAPER PILOT

THESIS

Presented to the Faculty of the School of Engineering
of the Air Force Institute of Technology

Air University

in Partial Fulfillment of the
Requirements for the Degree of
Master of Science

by

Robert P. Denaro

2 LT USAF

Garrison L. Greenleaf

2 LT USAF

Graduate Guidance and Control

October 1972

This document has been approved for public
release and sale; its distribution is unlimited.

Unclassified

DOCUMENT CONTROL DATA - R & D		
1. ORIGINATING ACTIVITY (Corporate author)		2a. REPORT SECURITY CLASSIFICATION
Air Force Institute of Technology (AFIT/EN) Wright Patterson AFB, Ohio 45433		Unclassified
2. REPORT TITLE		2b. GROUP
Selection of Optimal Stability Augmentation System Parameters for a High Performance Aircraft Using Fitch Paper Pilot		
4. DESCRIPTIVE NOTES (Type of report and inclusive dates)		
AFIT Thesis		
5. AUTHOR(S) (First name, middle initial, last name)		
Robert P. Denaro Garrison L. Greenleaf 2Lt. USAF 2Lt. USAF		
6. REPORT DATE	7a. TOTAL NO. OF PAGES	7b. NO. OF PAGES
17 October 1972	99	10
8a. CONTRACT OR GRANT NO.	8b. ORIGINATOR'S REPORT NUMBER(S)	
b. PROJECT NO. N/A	GGC/EE/73-3	
c.	9b. OTHER REPORT NO(S) (Any other numbers that may be assigned this report)	
d.	None	
10. DISTRIBUTION STATEMENT		
This document has been approved for public release and sale; its distribution is unlimited.		
Approved for public release; LAW AFR 190-17 Jerry C. Hix, Captain, USAF Director of Information		11. SPONSORING/MILITARY ACTIVITY
		Air Force Flight Dynamics Lab Wright Patterson AFB, Ohio (FDDC) 45433
13. ABSTRACT		
<p>Pitch Paper Pilot is a computer program which yields pilot parameters for a pitch tracking task and predicts the pilot rating of the aircraft handling qualities. Using Pitch Paper Pilot, optimal SAS gains are selected for the fixed form Stability Augmentation System of a high performance aircraft with structural bending. This aircraft was described in the Design Challenge to the 1970 Joint Automatic Control Conference. The final augmented aircraft responses compared favorably with desired normal acceleration response envelopes. The pilot model in Fitch Paper Pilot is modified in this study to include pilot lag and remnant which results in greater rating accuracy, although a few cases still show room for improvement.</p>		

DD FORM 1473

Unclassified

Security Classification

	ROLL	AT	PLC	AT	ROLL	AT
Pilot Model						
Pilot Rating						
Pilot Remnant						
Pitch Paper Pilot						
Pitch Tracking Task						
Stability Augmentation Systems						

Unclassified

Security Classification

Preface

This thesis was basically another in the series of studies that have been done on Paper Pilot. Captain Teddy L. Hollis used the same procedure in his thesis to design a SAS for the variable stability T-33. We used the Joint Automatic Control Conference Design Challenge aircraft as our subject, since it was a much tougher design problem for Paper Pilot.

Much time was spent in the first half of this study trying to modify Pitch Paper Pilot. Ron Anderson, of the Air Force Flight Dynamics Laboratory, had discovered that ratings were not very accurate for high natural frequency, low damped flight conditions. Following his suggestions, we added pilot lag and remnant to the pilot model in Pitch Paper Pilot, in an attempt to correct the deficiencies. Although accuracy was better; it was still not good enough to eliminate the problem. This plagued us once again in the Design Challenge work, where a poor design resulted for the high frequency, low damped case. We included some ideas for finally curing this problem in the "Recommendations for Future Study" section.

We wish to express deep appreciation to Major James Dillow, of the AFIT Math Department, for his constant help and advice during the course of this study. We also want to thank Mr. Ron Anderson of the AFFDL, for his valuable

GGC/EE/73-3

insights into our findings. Finally, we want to thank our advisor, Lt. Colonel Russel Hannen, for his support and advice throughout the study.

Additional thanks go to Mrs. Marilyn Baker for typing the final draft.

October 1972

Garry L. Greenleaf
Lieutenant USAF

Robert P. Denaro
Lieutenant USAF

Contents

Preface	iii
List of Figures	vii
List of Tables	x
List of Symbols	xi
Abstract	xiv
I. Introduction	1
Background	1
Paper Pilot	1
JACC Design Challenge	3
Problem Description	4
Approach	4
Overview	6
II. Pilot Rating Prediction	7
Introduction	7
Rating Expression	8
Shortcomings of the Original Program	9
Remnant Studies	9
New Pilot Model	10
Results of Remnant Studies	11
The Effect of Remnant	12
Modified Rating Expression	15
Final Modification to Paper Pilot	18
Calculation of Remnant	18
III. Joint Automatic Control Conference Design Challenge	21
Aircraft Dynamics	21
Measurement System and Structural Response Dynamics	23
Servoactuator	26
Design Specifications	26
IV. SAS Parameter Optimization	29
Brief Program Description	31
New A Matrix	32
Optimization Results	33
Gain Scheduling	39

Addition of Pre-Filter	41
Conclusions	45
V. Simulation	46
Procedure -- Commanded δ_c Response	46
JACC Design Challenge	
Response Envelopes	46
Normal Acceleration Response	48
Pre-Filter	48
High Frequency, Low Damping	50
Gust Response	52
Comparisons	53
VI. Conclusions	54
Recommendations for Future Study	55
Bibliography	56
Appendix A. System Equations in State Variable Form	58
Aircraft Equations of Motion	59
Servoactuator	60
Stability Augmentation System ...	60
Appendix B. State Equations from the Pilot Model	64
Time Delay	65
Lag-Lead Network	65
Pitch Command	66
Actuator Equation	66
Remnant	66
System Equations	67
Appendix C. Simulation Results	68
Flight Condition 1	70
Flight Condition 3	75
Flight Condition 5	80
Flight Condition 9	85
Flight Condition 13	91
Appendix D. Pre-Filter Equations	97

List of Figures

Figure	Page
1. Block Diagram of Closed Loop Aircraft	5
2. Block Diagram of New Pilot Model	11
3. Typical Remnant to Stick Ratio vs. Rating Curves for P Cases	16
4. Typical Remnant to Stick Ratio vs. Rating Curves for L Cases	17
5. Scatter Diagram for σ_r^2/σ_s^2 of 0.6	19
6. Design Challenge Normal Acceleration Response Envelopes	27
7. Detailed Block Diagram of Closed Loop System	30
8. "A" Matrix without Bending Modes	34
9. "A" Matrix with Bending Modes	35
10. K_q vs. $1/q$ for Optimal SAS	40
11. K_f vs. $1/q$ for Optimal SAS	40
12. Pre-Filter	42
13. Servoactuator Model	60
14. Open Loop Aircraft Response for Flight Condition 1	71
15. Closed Loop Aircraft Response for Flight Condition 1	72
16. Closed Loop Aircraft Response with Pre-Filter for Flight Condition 1; Break Frequency 5 rad/sec	73
17. Closed Loop Aircraft Response with Pre-Filter for Flight Condition 1; Break Frequency 2 rad/sec	74
18. Open Loop Aircraft Response for Flight Condition 3	76
19. Closed Loop Aircraft Response for Flight Condition 3	77

Figure	Page
20. Closed Loop Aircraft Response with Pre-Filter for Flight Condition 7; Break Frequency 5 rad/sec	78
21. Closed Loop Aircraft Response with Pre-Filter for Flight Condition 3; Break Frequency 2 rad/sec	79
22. Open Loop Aircraft Response for Flight Condition 5	81
23. Closed Loop Aircraft Response for Flight Condition 5	82
24. Closed Loop Aircraft Response with Pre-Filter for Flight Condition 5; Break Frequency 5 rad/sec	83
25. Closed Loop Aircraft Response with Pre-Filter for Flight Condition 5; Break Frequency 2 rad/sec	84
26. Open Loop Aircraft η_2 Response for Flight Condition 9	86
27. Open Loop Aircraft $\dot{\eta}_2$ Response for Flight Condition 9	87
28. Closed Loop Aircraft Response for Flight Condition 9	88
29. Closed Loop Aircraft Response with Pre-Filter for Flight Condition 9; Break Frequency 5 rad/sec	89
30. Closed Loop Aircraft Response with Pre-Filter for Flight Condition 9; Break Frequency 2 rad/sec	90
31. Open Loop Aircraft Response for Flight Condition 13	92
32. Closed Loop Aircraft Response for Flight Condition 13	93
33. Closed Loop Aircraft Response with Pre-Filter for Flight Condition 13; Break Frequency 5 rad/sec	94

Figure

Page

- 34. Closed Loop Aircraft Response with
Pre-Filter for Pilot Condition 13;
Break Frequency 2 rad/sec 95
- 35. Typical Aircraft Response to a
Specified Vertical Wind Gust 96

List of Tables

Table	Page
I. Cooper Pilot Rating Scale	2
II. Navy Data and Original Pitch Paper Pilot Predicted Ratings. Powered Approach Cases	13
III. Navy Data and Original Pitch Paper Pilot Predicted Ratings. Low Altitude, High Speed Cases	14
IV. Flight Conditions for Nominal Flight Path from Design Challenge	22
V. Discrete Stability Derivatives for the Design Challenge	24
VI. Optimum SAS Parameters, Actuator Rate, and Predicted Rating Using Ninth Order Model	36
VII. Actuator Rate and Predicted Rating Using the Thirteenth Order Model With SAS Parameters Found in the Ninth Order Optimization	37
VIII. Optimum Parameters for Selected Flight Conditions with the Thirteenth Order Model	38
IX. Actuator Rate and Predicted Rating for Model with Pre-Filter Using SAS Parameters from the Ninth Order Optimization	43
X. Comparison of Parameters for Flight Condition 1	44
XI. Comparison of Flight Conditions	47
XII. Short Period Parameters and Closed Loop Response Quality	51

List of Symbols

A	Matrix of Coefficients for State Vector Equation
g	Acceleration of Gravity (ft/sec^2)
k_j	Constants
K_p	Pilot Gain
K_n	SAS Gain for Normal Acceleration (rad/g)
K_q	SAS Gain for Pitch Rate ($1/\text{sec}$)
K_δ	SAS Gain for Elevator Deflection (Non-Dimensional)
L_z	Distance from Aircraft Center of Gravity to the Accelerometers (ft)
M_q	Pitch Moment Coefficients
M_w	
M_a	
M_{δ_e}	
n_z	Normal Acceleration (g 's)
n_{zf}	SAS Filter Normal Acceleration Output (g 's)
n_{zi}	Output of Normal Acceleration Sensor (g 's)
n_{zn}	Zero-Mean Gaussian White Noise Disturbance in Sensed Normal Acceleration (g 's)
n_{zss}	Steady-State Normal Acceleration (g 's)
PR	Pilot Rating
q	Pitch Rate (rad/sec)
q	Dynamic Pressure ($\frac{1}{2} \rho U_0^2$) (psf)
q_f	SAS Filter Pitch Rate Output (rad/sec)
q_i	Output of Pitch Rate Sensor (rad/sec)
q_n	Zero-Mean Gaussian White Noise Disturbance in Sensed Pitch Rate (rad/sec)
r	Time Derivative of First Bending Mode Deflection (ft/sec)

s	Time Derivative of Second Bending Mode Deflection (ft/sec); Also Laplace Operator
t	Time (sec)
T_e	Actuator Time Constant (sec)
T_I	Pilot Lag Time Constant (sec)
T_L	Pilot Lead Time Constant (sec)
U_o	Nominal Aircraft Airspeed (ft/sec)
w	$w = U_o \alpha$ (rad-ft/sec)
w_g	Vertical Wind Gust (ft/sec)
\bar{x}	Feedback State Vector
y_j	Pilot Model Variables
z	System State Vector
z_a	Normal Force Coefficients
z_{δ_e}	
α	Angle of Attack (rad)
β	SAS Feedback Variable (rad)
δ	Pilot Model Output Less Remnant (rad)
δ'	Output of Lag-Lead Portion of Pilot Model (rad)
δ_e	Elevator Deflection (rad)
δ_p	Pilot Model Output (rad)
δ'_p	Output of Pre-Filter (rad)
δ_r	Remnant Input (rad)
δ_s	SAS Output (rad)
δ_e	Error Signal to Servoactuator (rad)
ζ	Aircraft Short Period Damping
ζ_j	Damping Constant of jth Bending Mode
ζ_i	Zero-Mean Gaussian White Noise Input (rad)

ξ_n	Zero-Mean Gaussian White Noise Remnant Input (rad)
ρ	Atmospheric Density (slug/ft ³)
θ	Pitch Attitude (rad)
θ_c	Commanded Pitch Input (rad)
θ_e	Pitch Error Signal To Pilot (rad)
δ_{nj}	Relative Displacement at Accelerometers due to jth Bending Mode (ft)
$\lambda_{\theta j}$	jth Bending Mode Slope at Sensor Location Relative to Generalized Displacement u_j (rad/ft)
u_j	jth Bending Mode Deflection at a Specific Reference Station
σ_c^2	Commanded Input Variance (rad ²)
σ_i^2	Input Variance (rad ²)
σ_r^2	Remnant Variance (rad ²)
σ_s^2	Stick Input Variance (rad ²)
σ_e^2	Pitch Error Variance (rad ²)
τ	Time Constant (sec)
ψ	Forcing Function Coefficient for Bending Modes (ft/sec ²)
ω	Frequency (rad/sec)
ω_j	Frequency of jth Bending Mode (rad/sec)
ω_c	Frequency of Wind Gust Power Spectral Density (rad/sec)
ω_f	Break Frequency of SAS Filter (rad/sec)
ω_p	Break Frequency of Pre-Filter (rad/sec)
ω_n	Aircraft Short Period Natural Frequency (rad/sec)
ω_r	Remnant Break Frequency (rad/sec)

SELECTION OF OPTIMAL STABILITY AUGMENTATION SYSTEM PARAMETERS
FOR A HIGH PERFORMANCE AIRCRAFT USING PITCH PAPER PILOT

I. Introduction

Background

The study of pilot-vehicle systems has been the subject of extensive research in recent years. Examining aircraft handling qualities as a closed-loop system, with the pilot in the control loop, promises to give more accurate evaluation of aircraft flying qualities than previous evaluations of the open-loop aircraft alone. Most of the effort has been devoted to developing an accurate human pilot model - not an easy task, since the human being is probably the most sophisticated and complex control system in existence.

Pilot opinion rating has also received much attention, notably in studies by Cooper (3:--). A rating scale for pilot opinion of aircraft flying qualities was developed from Cooper's work, and has now been fairly well standardized for flight test and research. The Cooper Rating Scale, shown in Table 1 on the next page, is a numerical scale from 1 to 10, where a rating of 1 indicates excellent flying characteristics and a rating of 10 indicates a totally unflyable aircraft.

Paper Pilot. In 1970, Anderson, Connors and Dillow (1:--) developed a promising new technique of closed-loop pilot-vehicle analysis for pitch tracking tasks, a computer

TABLE 1
COOPER PILOT RATING SCALE

Operating Conditions	Adjective Rating	Numerical Rating	Description	Primary Mission Accomplished	Can Be Landed
Normal Operation	Satisfactory	1	Excellent, includes optimum	Yes	Yes
		2	Good,	Yes	Yes
		3	Satisfactory, but with some mildly unpleasant characteristics	Yes	Yes
Emergency Operation	Unsatisfactory	4	Acceptable, but with unpleasant characteristics	Yes	Yes
		5	Unacceptable for normal operation	Doubtful	Yes
		6	Acceptable for emergency condition only*	Doubtful	Yes
No Operation	Unacceptable	7	Unacceptable even for emergency condition*	No	Doubtful
		8	Unacceptable - dangerous	No	No
		9	Unacceptable - uncontrollable	No	No
	Catastrophic	10	Motions possibly violent enough to prevent pilot escape	No	No

*Failure of a stability augments

program called "Pitch Paper Pilot". This program was an extension of prior work called "Paper Pilot" (2:--), a VTOL hover tracking task study. Pitch Paper Pilot is a fully automated procedure that predicts pilot-vehicle performance and a pilot opinion for the pitch tracking task, based on the assumption that a pilot adjusts his parameters to minimize his numerical rating of the aircraft dynamics.

In 1971, Hollis (3:--) used the Paper Pilot program as a design tool to design an aircraft stability augmentation system (SAS) and optimize its gains to minimize the pilot rating of the aircraft at given flight conditions. The subject aircraft was a variable stability T-33, an aircraft not capable of an extreme range of either Mach number or dynamic pressure.

JACC Design Challenge. At the 1970 Joint Automatic Control Conference, Rediess and Taylor posed a flight control system design challenge for a hypothetical aircraft with extreme variations in flight conditions (7:--). The challenge was to design a SAS for this aircraft, whose flight envelope included Mach numbers from 0.35 to 3.00 and dynamic pressures ranging from 150 psf to 1500 psf. The aircraft also has structural flexibility represented by its first two bending modes. This problem was dealt with by Sherrard (8:--), using optimal control, Ward (9:--), using classical control, and Paul (6:--), using self-adaptive control techniques.

Problem Description

The problem for this study was to design a stability augmentation system for the JACC Design Challenge Aircraft. The closed loop aircraft response was compared with desired response envelopes as given in the Design Challenge. These envelopes specified limits on the normal acceleration and the derivative of normal acceleration responses. Also, there was a numerical limit on the rms wind gust response to a specified input.

Approach

The method used to design the SAS was basically the Pitch Paper Pilot SAS optimization technique developed by Hollis. The entire closed loop system is shown in Figure 1. The optimization of the SAS was fixed-form, that is, only the values of feedback gains within the SAS were optimized with respect to pilot rating. The SAS gains were systematically changed until a minimum aircraft closed loop pilot rating was obtained. Those final gains, then, were the optimal SAS gains. This was done for each of a set of discrete flight conditions which represented the entire flight envelope. The feedback vector, \bar{x} , included elevator deflection, δ_e , pitch rate, q , and normal acceleration, n_z . The fixed form pilot model

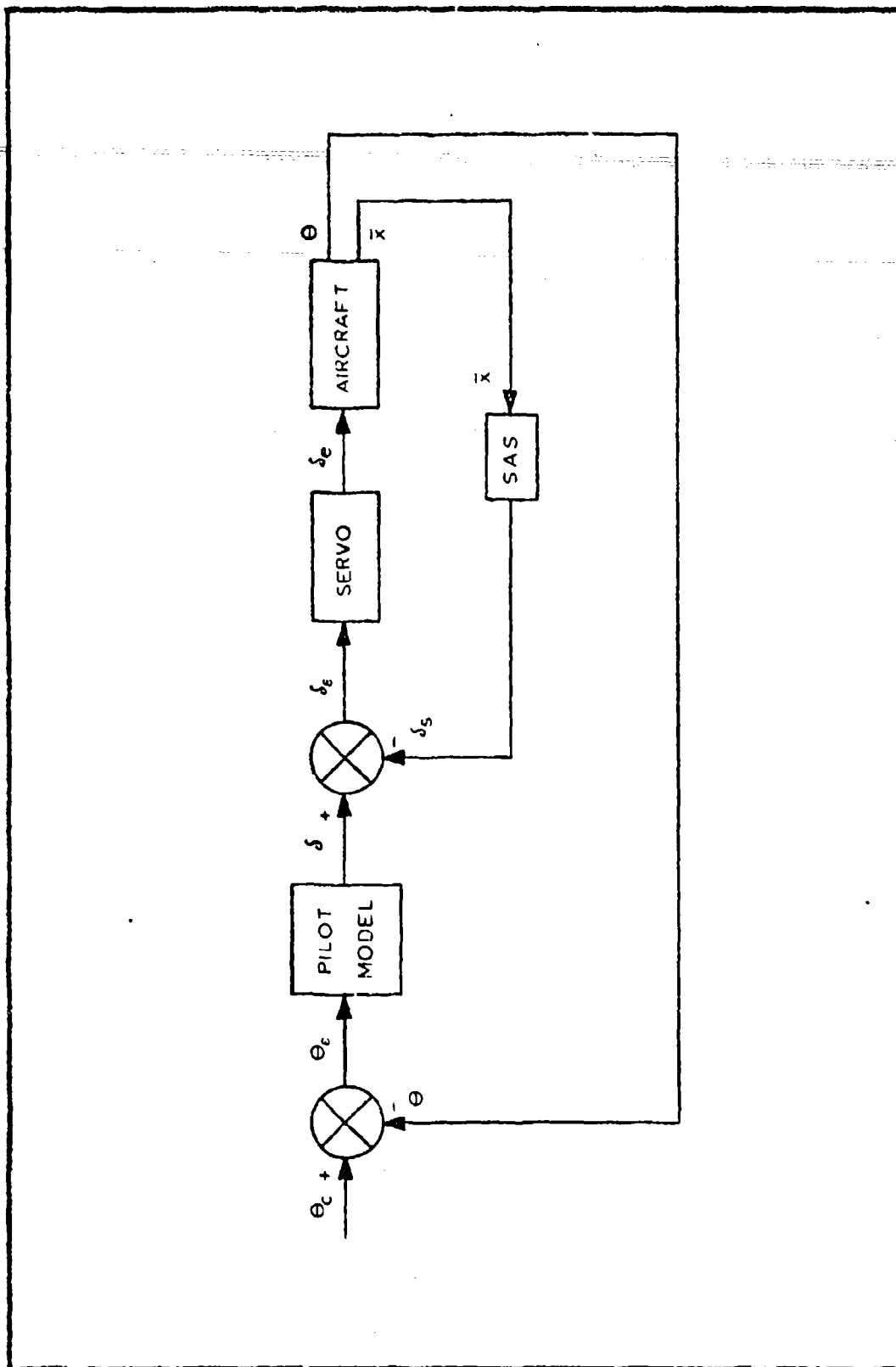


Figure 1. Block Diagram of Closed Loop Aircraft

was part of the Pitch Paper Pilot routine, which produced pilot ratings for the particular closed loop dynamics in use. Before this technique could be used, however, certain modifications to Paper Pilot were necessary.

As noted by Anderson (1:12), Pitch Paper Pilot did not yield accurate pilot ratings for an aircraft with high short period natural frequency and low damping. In this study, pilot lag and remnant were added to the pilot model in an attempt to make Paper Pilot ratings correlate with actual pilot ratings for aircraft with these short period parameters. The level of remnant was adjusted to better match predicted pilot ratings to actual pilot ratings.

Overview

Since the first part of this investigation concerned modifications to Pitch Paper Pilot without considering the JACC Design Challenge, these modifications were discussed in Chapter II. The JACC Design Challenge is introduced in Chapter III, and the digital optimization of SAS gains is summarized in Chapter IV. Analog simulation results are the topic of Chapter V, and in Chapter VI some conclusions on the entire study are drawn and recommendations offered for future study.

II. Pilot Rating Prediction

Introduction

Pilot Rating prediction for this study is based on a modified version of the "Pitch Paper Pilot" computer program, originally developed by Anderson, Dillow and Connors (1:--). This program determines the pilot model parameters, closed loop pilot-vehicle performance, and a Cooper scale pilot opinion rating of the aircraft's handling qualities for a pitch tracking task.

As originally formulated, this program used a simple pilot model, incorporating gain, lead, and a pure time delay. The time delay accounted for both neuro-muscular lag and reaction time delay. As shown in Figure 1, combining this pilot model with the SAS, airframe, and elevator servo models results in a complete closed loop pilot-vehicle model, which is used to define a set of state equations used in the program.

The procedure for predicting ratings from this closed loop formulation is based on the hypothesis that a human pilot will adjust his parameters (the equivalent of the pilot model gain, lead and time delay) to allow him to give the lowest (best) rating to the aircraft that he can at the particular flight condition. Thus,

by minimizing some properly chosen rating expression with respect to pilot parameters, the program can be expected to produce ratings well correlated with actual pilot ratings. In the original program, an empirically developed rating function, PR, is minimized with respect to K_p , the gain of the pilot in the pitch loop, and T_L , the pilot lead in the pitch loop (the time delay is considered a constant). Conjugant gradient and Newton-Raphson search procedures, as shown in Hollis (3:17-23), were used to find the minimum.

Rating Expression. Anderson, Dillow and Connors (1:4-5) developed a rating expression for use with the above procedure. This expression is of the form

$$PR = W_1 + W_2 + 1.0 \quad (1)$$

where

$$W_1 = \frac{0.1 \sigma_c}{0.974 \sigma_c - \sigma_e} \quad \sigma_e < 0.974 \sigma_c \quad (2)$$

and

$$W_2 = \begin{cases} -2.5 T_L & T_L < 0 \\ 2.5 T_L & 0 \leq T_L \leq 1.3 \\ 3.25 & T_L > 1.3 \end{cases} \quad (3)$$

W_1 is a measure of closed loop performance where σ_c^2 is the commanded input variance and σ_e^2 is the pitch error variance. W_2 is a measure of pilot workload, and is a function of T_L , the pilot lead.

Shortcomings of the Original Program. As originally formulated, Pitch Paper Pilot gave accurate ratings for most flight conditions. However, when the program was applied to flight conditions with high short period frequency and low damping, the predicted ratings for the flight conditions were significantly better (lower) than actual ratings (1:12).

Since the Paper Pilot concept does work very well for most pitch cases and for all flight conditions when applied to other tasks, such as roll (5:--) and hover tracking (2:--), some modification to Pitch Paper Pilot should correct this fault.

Remnant Studies

One possible approach to improving the rating scheme is to include pilot remnant in the pilot model. Remnant is that portion of a pilot's output that is not linearly correlated with the system input (4:--). Pure noise injection by the pilot, non-linear operations, and non-steady pilot behavior are considered to be the possible sources of remnant.

It was hypothesized that the addition of remnant to the pilot model would tend to produce higher ratings from Pitch Paper Pilot for all flight conditions, but that this effect would be greater for conditions with low

damping and high frequency. This would allow the critical (high frequency, low damping) predicted ratings to be raised to more realistic values without pushing other cases too far above their original values.

Considering remnant as pilot induced noise with a relatively high bandwidth, it is easy to see that this pilot noise could excite an undesired response in the aircraft. An aircraft with a high short period natural frequency should filter less of this remnant effect out, resulting in greater tracking error. If this undesired response were also lightly damped, it would be even more noticeable to the pilot. Thus, for the critical case, tracking error and pilot workload would increase more than for other cases. For a pilot model with remnant, therefore, predicted ratings would be expected to increase by a greater amount for the critical case than for other cases.

New Pilot Model. To test this hypothesis, a new pilot model was used in the computer program which was a higher order model including both remnant and a lag term. The new pilot model is shown in Figure 2. Note that the remnant is modeled as a zero-mean gaussian white noise put through a first order filter. To model high frequency remnant, the cut-off frequency, ω_c , was chosen as 20 radians per second. T_I is the lag time constant, which was chosen as a constant of 0.1 seconds to represent the neuro-muscular

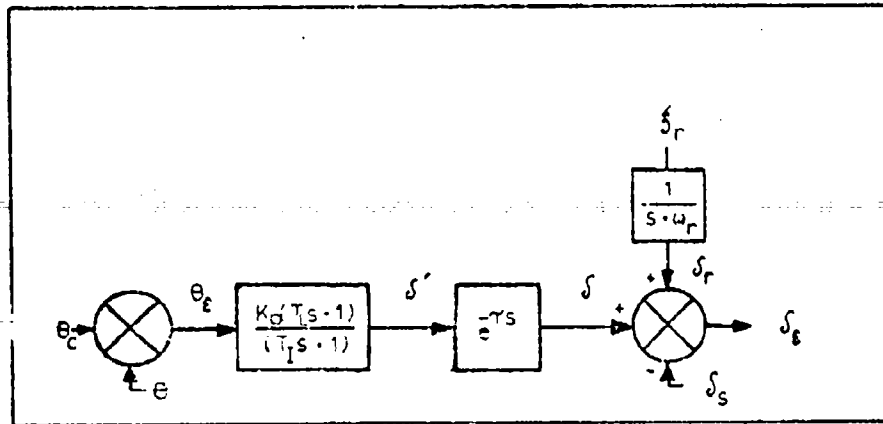


Figure 2. Block Diagram of New Pilot Model.

lag. τ in the time delay term was reduced to 0.32 seconds, representing the higher order neuro-motor delay and the pure time delay. The program still optimizes with respect to K_D and T_L only.

A set of system equations for this pilot model, including the actuator, are developed in Appendix B. By combining these equations with the longitudinal airframe and control system equations of Appendix A and reducing them to state variable form, an accurate mathematical model of the closed-loop system was substituted into the proper sub-routines of the original Pitch Paper Pilot. This modified program was then used to test the effect of the remnant on rating predictions.

Results of Remnant Studies

The modified Pitch Paper Pilot program was tested on cases for which real ratings were known. The data from a

series of Navy tests with a variable stability F-8 (1:10-12) were used as test cases. Pertinent data for these two sets of cases, one set for landing approach and one for low altitude high speed tests, are shown in Tables II and III on the following pages. Also included in the Tables are the actual average pilot rating. As can be seen from Table III, the agreement between actual and predicted ratings is particularly poor for the low altitude high speed cases. These cases are mainly of the high frequency, low damping type. For the other cases, as shown in Table II, Paper Pilot did give good results.

The Effect of Remnant. Using the new Pitch Paper Pilot, a series of predicted pilot ratings were computed for each flight condition using a variety of different levels of remnant, starting, in each case, with a zero remnant. A commanded input with an rms value of 0.5 radians was used in all cases. With this input and the remnant specified, stick input could be calculated for each flight condition and remnant level.

Remnant only begins to affect ratings as it becomes significant in comparison to the stick input required for the particular flight condition. For this reason, the set of ratings for each flight condition were plotted with respect to the remnant to stick ratio (σ_r^2 / σ_s^2).

TABLE II. Navy Data and Original Pitch
Paper Pilot Predicted Ratings.
Powered Approach Cases.

Reference 1.

NAVY CASE	CONFIGURATION		PILOT RATING	PREDICTED RATING
	ω_n	ξ		
PA	2.15	0.42	3.50	3.27
PB	3.04	0.77	3.70	2.83
PC	1.53	0.20	5.75	4.85
PD	1.60	0.29	4.25	4.12
PE	1.69	0.37	2.67	3.75
PF	1.77	0.43	2.50	3.51
PG	1.21	0.30	5.00	4.99
PH	1.28	0.40	4.17	4.37
PJ	1.53	0.68	2.50	3.59
PK	1.00	0.39	7.00	5.58
PL	1.34	0.80	3.25	3.84

- a. Average pilot rating for the test aircraft at the given flight condition. Individual pilot's ratings varied as much as three ratings for some of the flight conditions.
- b. Ratings calculated from the original Pitch Paper Pilot program.

TABLE III. NAVY DATA AND ORIGINAL PITCH
PAPER PILOT PREDICTED RATINGS.
LOW ALTITUDE, HIGH SPEED CASES.

Reference 1.

Navy Case	Configuration		Pilot Rating IR^a	Predicted Rating R^b
	ω_n	ξ		
LA	13.8	0.18	4.00	2.18
LB	14.7	0.28	2.50	2.25
LC	15.0	0.30	2.25	2.42
LD	9.3	0.32	4.00	2.17
LE	9.4	0.35	3.60	2.18
LF	9.8	0.41	2.63	2.24
LG	10.4	0.45	1.33	2.34
LH	5.3	0.20	5.33	2.83
LJ	4.8	0.30	4.00	2.66
LK	4.6	0.37	4.00	2.63
LL	4.0	0.41	4.17	2.62

- a. Average pilot rating for the test aircraft at the given flight condition. Individual pilot's ratings varied as much as three ratings for some flight conditions.
- b. Ratings calculated from the original Pitch Paper Pilot program.

Plots of remnant to stick ratio versus predicted rating are very similar for all cases; the predicted rating rises by approximately the same amount for a given remnant to stick ratio, no matter what the flight condition. Four typical cases are shown in Figures 3 and 4. They clearly show this similarity of curves for different flight conditions.

This similarity in remnant effects makes it impossible to pick a particular remnant to stick ratio that would increase the ratings for the critical case (high frequency, low damping) without increasing the ratings in the other cases by about the same amount. Thus, the critical cases could not be adjusted to more closely correlate with real pilots' ratings without having a corresponding effect of increasing the other ratings to values that were significantly higher than their actual ratings.

Modified Rating Expression

Including remnant in the pilot model failed to provide the anticipated improvement in Pitch Paper Pilot, so modification of the rating expression was tried. Small adjustments were made to the constants in the pilot rating expression in an attempt to correct the critical ratings. This modification also failed to solve the problem. Each flight condition was similarly affected by equal changes in constants, as with the remnant effects.

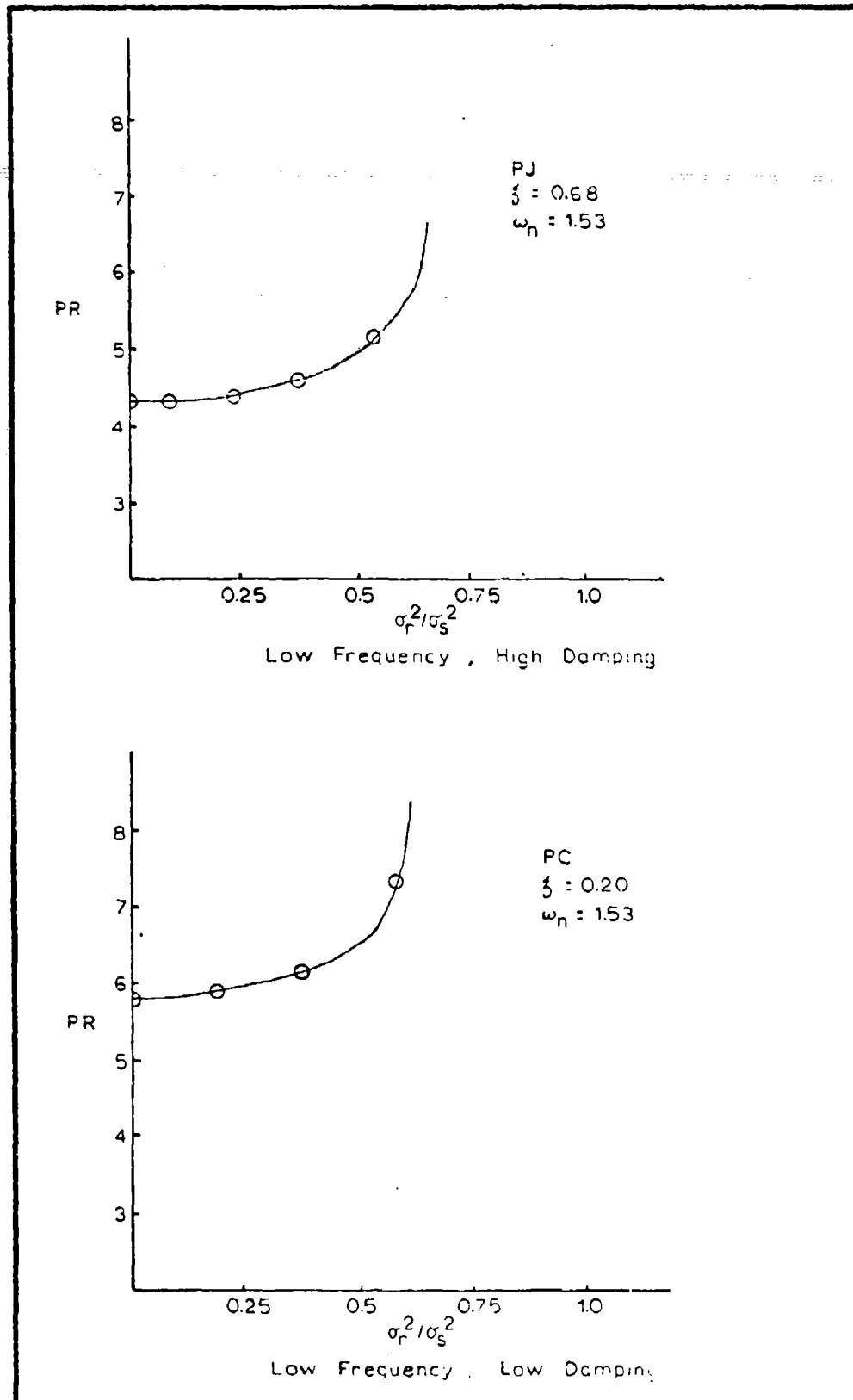


Figure 3. Typical Remnant to Stick Ratio vs. Pilot Rating Curves for 1 rad/s.

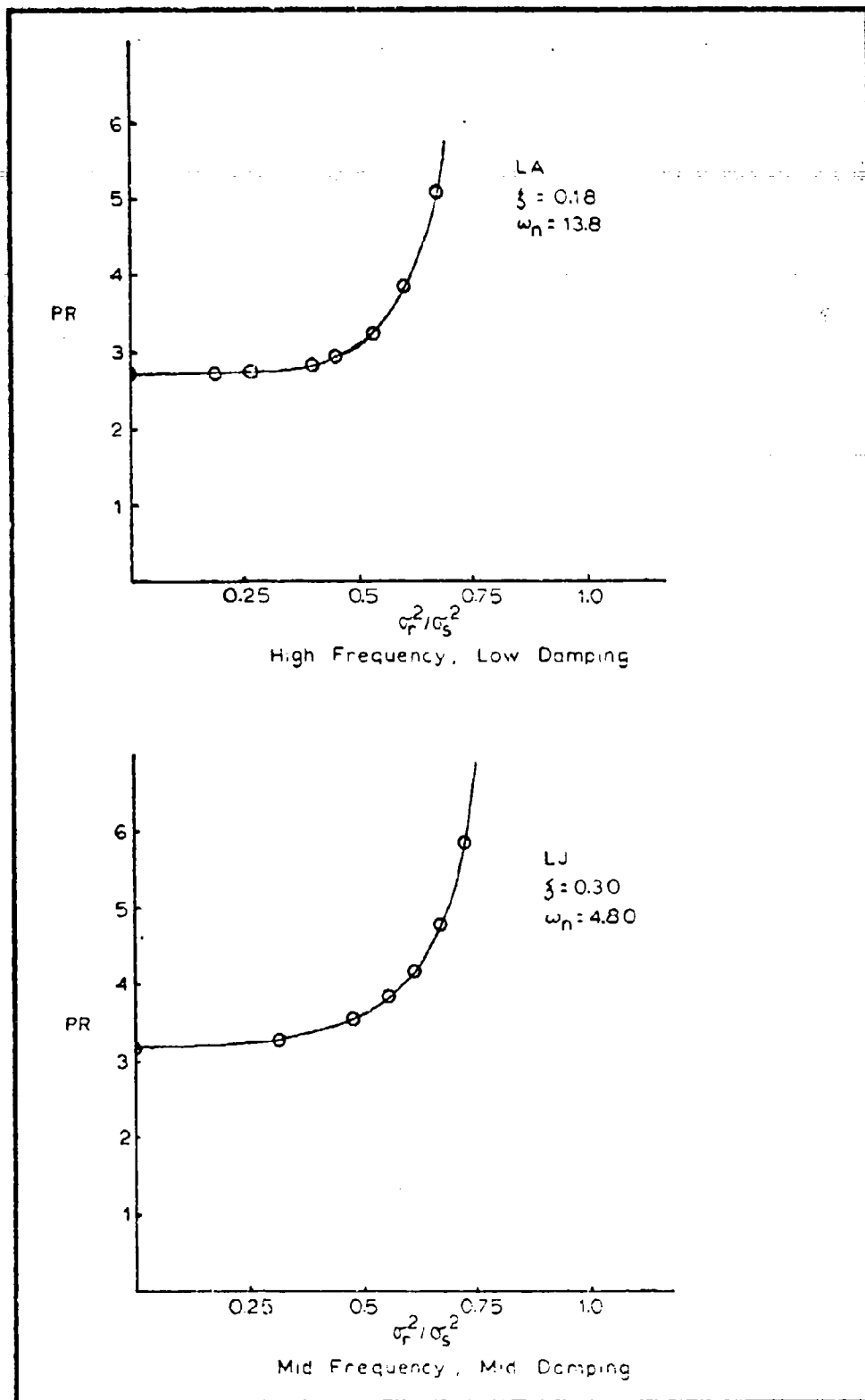


Figure 4. Typical Remnant to Stick Ratio vs. Pilot Rating Curves for L Cases.

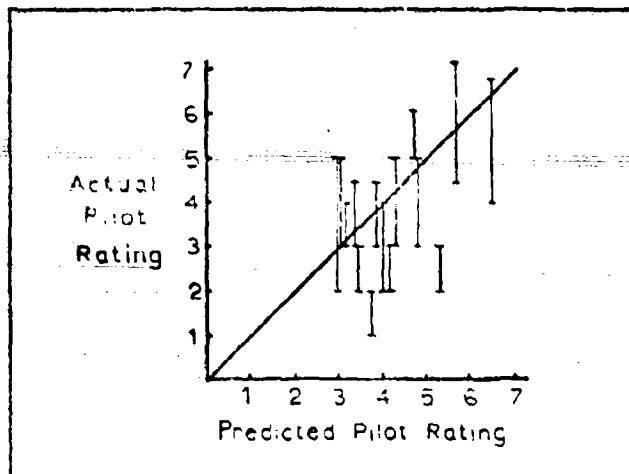
Final Modification to Paper Pilot

Obviously, the changes made in the original program were not very successful in eliminating Paper Pilot's main fault, inaccurate ratings for high frequency, low damping conditions. However, the modified pilot model, with remnant and lag, was incorporated in the closed-loop model because this model is a closer approximation to the human pilot and the use of a non-zero remnant did slightly improve the predicted rating for the critical flight conditions.

A remnant to stick ratio of 0.6 was selected for the revised model. This ratio is in a region that does not cause extremely large changes in rating for small changes in the remnant to stick ratio. The scatter diagram of actual versus predicted pilot rating for this value of remnant to stick ratio, as shown in Figure 5, does show a fair correlation of actual to predicted pilot rating. The 0.6 remnant to stick ratio did give the best scatter diagram of the ratios tested.

Calculation of Remnant. The remnant required to generate the proper remnant to stick ratio is calculated by a simple procedure incorporated in the computer program. Mean-square remnant value is determined by manipulating the following equation

$$\sigma_s^2 = k_1 \sigma_i^2 + k_2 \sigma_r^2 \quad (4)$$

Figure 5. Scatter Diagram for σ_r^2/σ_s^2 of 0.6.

where σ_i^2 is the mean-square input. First, k_1 is found by setting the remnant at zero ($\sigma_r = 0$) so that

$$k_1 = \frac{\sigma_s^2}{\sigma_i^2} \quad (5)$$

then k_2 is found by setting the remnant at unity and the input to zero ($\sigma_i = 0$) so that

$$k_2 = \sigma_s^2 \quad (6)$$

Now, for a specified remnant to stick ratio, k_3 ,

$$\sigma_r^2(1/k_3) = k_1 \sigma_i^2 + k_2 \sigma_r^2 \quad (7)$$

and

$$\sigma_r^2 = \frac{k_1 \sigma_i^2}{(1/k_3) - k_2} \quad (8)$$

This routine was added to Pitch Paper Pilot and the modification was used in the optimization routine.

Though the modifications were not totally successful,
the resultant Pitch Paper Pilot, including remnant, was an
improvement, and assumed to be a good tool for SAS design.

III. Joint Automatic Control Conference Design Challenge

The JACC Design Challenge (7:--) specified aircraft dynamics, servoactuator dynamics, onboard measurement systems, structural response dynamics, a mission profile, a gust environment, and desired closed loop responses for the final augmented aircraft design. The aircraft was to be piloted by a human pilot through the mission profile. Sixteen discrete points in the mission profile were selected as representative of the entire flight envelope. These flight conditions are listed in Table IV. The problem was to design a SAS for this aircraft which brought the aircraft response in all flight conditions to within the specified envelopes.

Aircraft Dynamics

Only the longitudinal mode of the aircraft was considered. The phugoid mode was assumed to be negligible. The longitudinal short period rigid body dynamics of the basic aircraft are given by the following set of linearized differential equations

$$\dot{\alpha} = Z_{\alpha} \alpha + \dot{q} + Z_{\delta_e} \delta_e + Z_{\alpha} \frac{w_g}{U_0} \quad (9)$$

$$\dot{q} = M_{\alpha} \alpha + M_{\dot{q}} \dot{q} + M_{\delta_e} \delta_e + M_{\alpha} \frac{w_g}{U_0} \quad (10)$$

$$n_z = \frac{U_0}{g} (q - \dot{\alpha}) \quad (11)$$

TABLE IV. FLIGHT CONDITIONS FOR NOMINAL
FLIGHT PATH FROM DESIGN CHALLENGE.

Reference 7.

Flight ^a Condition	Mach Number	Velocity (fps)	Altitude (ft)	Dynamic Pressure (psf)
1	0.35	391	0	150
2	0.63	704	0	490
3	0.86	961	0	830
4	1.03	1151	0	1160
5	1.14	1272	0	1500
6	1.60	1670	18,500	1500
7	2.07	2046	31,500	1500
8	2.54	2460	41,000	1500
9	3.00	2904	50,000	1500
10	3.00	2904	55,000	1155
11	3.00	2904	62,000	820
12	3.00	2904	74,000	490
13	3.00	3020	101,000	150
14	2.33	2285	88,500	150
15	1.68	1626	73,000	150
16	1.01	987	52,000	150

- a. Flight conditions are picked along the nominal trajectory at fifteen second intervals, with Flight Condition 1 at zero time.

where α is angle-of-attack, q is pitch rate, δ_e is elevator deflection, w_g is a wind gust, U_0 is nominal airspeed, g is the acceleration of gravity and the coefficients of these variables are the aircraft stability derivatives. These equations are transformed into a state variable form used in this study in Appendix A.

In the Design Challenge, the stability derivatives were expressed statistically as random variables with a normal distribution. However, to narrow the design problem, only the mean values of the stability derivatives were used in this study. They are listed in Table V. The original statistical description of these coefficients can be found in the JACC Design Challenge (7:18).

Measurement System and Structural Response Dynamics

The effect of the structural response on the feedback system is a function of the sensor locations. Only the first two bending modes were considered, modeled by the differential equations

$$\ddot{u}_1 + 2\zeta_1\omega_1\dot{u}_1 + \omega_1^2 u_1 = \psi\delta_e \quad (12)$$

$$\ddot{u}_2 + 2\zeta_2\omega_2\dot{u}_2 + \omega_2^2 u_2 = \psi\delta_e \quad (13)$$

where $\psi = -4U_0 Z_{\delta_e}$ and u_1 and u_2 are the first and second bending mode deflections respectively, at a specific reference station. Again, although the original Design

TABLE V. DERIVATIVES OF THE DERIVATIVES
FOR THE CIRCULAR ORBIT.

Flight Condition	Z_m (1/sec)	Z_{j_0} (1/sec)	K_m (1/sec ²)	K_{j_0} (1/sec ²)	K_q (1/sec)
1	-0.300	-0.112	-1.500	-6.000	-0.300
2	-0.980	-0.442	-4.900	-19.600	-0.980
3	-1.660	-0.490	-15.770	-33.200	-1.660
4	-2.275	-0.459	-46.052	-45.878	-2.275
5	-2.727	-0.163	-57.900	-51.850	-2.727
6	-1.830	-0.465	-51.000	-46.500	-1.830
7	-1.018	-0.759	-43.950	-35.925	-1.018
8	-0.807	-0.254	-36.000	-25.350	-0.807
9	-0.600	-0.150	-30.000	-15.000	-0.600
10	-0.462	-0.116	-23.100	-11.550	-0.462
11	-0.328	-0.082	-16.400	-8.200	-0.328
12	-0.196	-0.049	-9.800	-4.900	-0.196
13	-0.060	-0.015	-3.000	-1.500	-0.060
14	-0.010	-0.030	-4.005	-3.002	-0.010
15	-0.167	-0.015	-4.900	-1.470	-0.167
16	-0.298	-0.010	-5.905	-5.978	-0.298

Challenge presented the bending mode parameters in a statistical sense, only the mean values were used in this study. These are

$$\omega_1 = 30 \text{ rad/sec} \quad \xi_1 = 0.01 \quad (14)$$

$$\omega_2 = 50 \text{ rad/sec} \quad \xi_2 = 0.01$$

The measurement sensors were assumed to be ideal, however, the quantities measured included the bending mode response and independent noise in addition to the rigid body response. The following measurements were used for the selected SAS configuration

$$q_i = q - \lambda_{\theta_1} \dot{v}_1 - \lambda_{\theta_2} \dot{v}_2 + q_n \quad (15)$$

$$n_{z_i} = n_z + \frac{1}{g} (L_z a + \phi_{n_1} \ddot{v}_1 + \phi_{n_2} \ddot{v}_2) + n_{z_n} \quad (16)$$

These are the indicated pitch rate and indicated normal acceleration equations. λ_{θ_1} and λ_{θ_2} are the respective bending mode slopes at the sensor locations relative to the generalized displacements, v_1 and v_2 , while ϕ_{n_1} and ϕ_{n_2} are the relative displacements at the accelerometers due to the bending modes. L_z is the distance from the aircraft center of gravity to the accelerometers. The terms n_{z_n} and q_n are zero mean gaussian white noise. The values of the parameters used are

$$\lambda_{\theta_1} = -0.025 \text{ rad/ft.}$$

$$\lambda_{\theta_2} = 0.040 \text{ rad/ft.}$$

$$L_z = 10 \text{ ft.}$$

$$\phi_{n_1} = -0.15$$

$$\phi_{n_2} = 0.45$$

$$E(q_n)^2 = (0.0005)^2 (\text{rad/sec})^2$$

$$E(n_{z_n})^2 = (0.01)^2 (g)^2$$

Servoactuator

The control servoactuator is described by a first order lag with an output rate limit. The equation for the servoactuator is

$$\dot{S}_e = -20 S_e + 20 S_r \quad (17)$$

with a rate limitation of

$$|\dot{S}_e| \leq 0.5 \text{ rad/sec} \quad (18)$$

where S_r is a commanded input to the servoactuator.

Design Specifications

The design specifications from the Design Challenge are the response envelopes shown in Figure 6. These are the envelopes superimposed on the plots of the aircraft responses shown in Appendix C. The response envelopes for normal acceleration and its derivative are normalized in amplitude by the steady state normal acceleration

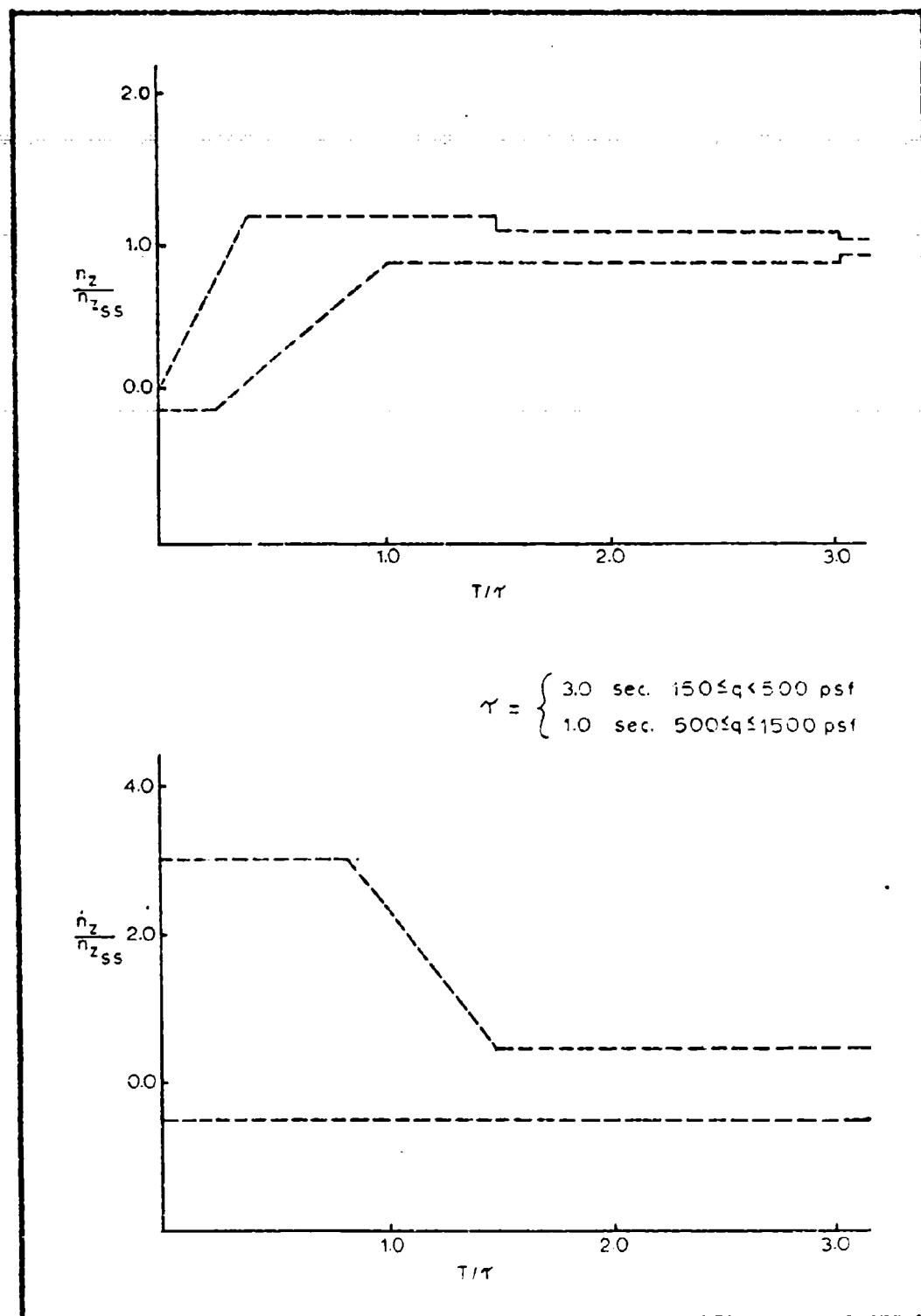


Figure 6. Design Challenge Normal Acceleration Response Envelopes.

and in time by a factor τ which is a discrete function of dynamic pressure

$$\tau = 3.0 \text{ sec} \quad 150 \leq q < 500 \text{ psf}$$

$$\tau = 1.0 \text{ sec} \quad 500 \leq q \leq 1500 \text{ psf}$$

In the absence of a pilot input, the aircraft response to a specified vertical wind gust must be less than 0.1 g rms. The wind gust, w_g , is assumed to have a zero-mean gaussian distribution, and a power spectral density given by

$$G_w(\omega) = \frac{2}{\pi} \frac{\sigma^2 \omega_c}{\omega^2 + \omega_c^2} \quad (19)$$

where $\sigma = 5.0$ fps and $\omega_c = U_0/1000$ rad/sec.

Finally, the Design Challenge specified restrictions on stick force, but this requirement was not considered in this study. It was assumed that stick force could be artificially induced, and would not limit the SAS design involved in this study.

IV. SAS Parameter Optimization

Designing a stability augmentation system for the JACC Design Challenge aircraft was the main project for this study. This was done by changing the feedback gains for a specified fixed form SAS until the closed loop system, including the pilot, actuator and SAS, as well as the aircraft dynamics, had the lowest pilot rating. This optimum pilot rating was determined by Pitch Paper Pilot.

The design was restricted to the longitudinal axis, for a pitch tracking task. A detailed diagram of the closed loop system model is shown on the following page, Figure 7. Note that the stability augmentation system used the three parameters; elevator deflection, δ_e , pitch rate, q , and normal acceleration, n_z . As discussed in Chapter III, measurements of n_z and q are subject to disturbance by the aircraft structural bending. For this reason, these measurements are filtered in the feedback loop, to remove some of this disturbance.

For this aircraft, the break frequency of the filter was chosen as 8. This was the value arrived at by Sherrard, and represented a good choice of maximum attenuation of body bending effects with minimum attenuation of the rigid body dynamics (8:28).

The pilot model for the closed loop system is the new pilot model developed for Pitch Paper Pilot in Chapter II. The servoactuator dynamics are represented by a simple first order lag.

Brief Program Description

Pitch Paper Pilot uses the closed loop system model to determine the aircraft's predicted pilot rating. A pattern search technique, developed by Zuckerman (10:--), uses Pitch Paper Pilot to find the SAS gains that minimize predicted pilot rating within the actuator rate constraints given in Chapter III.

The procedure is as follows: SAS gains are changed systematically and Pitch Paper Pilot computes a predicted pilot rating for each set of gains. The program proceeds until a set of gains is found that give a minimum predicted rating, without allowing the quantity, $\sigma_{\dot{\delta}_e}$, to exceed 0.5 radians per second. $\sigma_{\dot{\delta}_e}$ is a three sigma measure of elevator rate, so there is only a very low probability that the rate constraints would be violated if $\sigma_{\dot{\delta}_e}$ is kept within limits.

This SAS optimization technique is basically the same as that used by Hollis in his study of the variable stability T-33 (3:25-31).

New A Matrix. Pitch Paper Pilot requires the closed loop system to be modeled in a state vector equation form.

This is written as

$$\dot{z} = Az + v \quad (20)$$

where z is the state vector, v is a noise vector and A is a matrix of coefficients called the A matrix.

In examining the Design Challenge aircraft, two closed loop models were used, one of ninth order without the two second order structural bending modes and one of thirteenth order including the bending modes. The state equations for these two models are developed in detail in Appendices A and B.

The form of the state vector, z , for ninth or thirteenth order is as shown below.

$$z = \begin{bmatrix} \theta \\ q \\ \beta \\ w \\ \delta_c \\ y_1 \\ y_2 \\ \theta_c \\ \delta_r \end{bmatrix} \quad \text{or} \quad \begin{bmatrix} \theta \\ q \\ \beta \\ w \\ \delta_e \\ y_1 \\ y_2 \\ \theta_c \\ \delta_r \\ v_1 \\ v_2 \\ r \\ s \end{bmatrix} \quad (21)$$

The two vectors are similar, except that the thirteenth order includes four extra states to represent the bending modes. θ is the pitch. $\dot{\theta}$ is pitch rate. β is a feedback state combining vertical acceleration and pitch rate feedback ($\beta = K_q \dot{\theta}_f + K_{n_z} n_{z_f}$). w is a state formed from angle of attack and true airspeed ($w = U_0 \alpha$). δ_e is the actuator (elevator) deflection. y_1 and y_2 are states formed from the lag-lead and time delay portions of the pilot model, as detailed in Appendix B. θ_c is the pitch command. δ_r is the remnant. v_1 and v_2 represent the longitudinal bending terms for the JACC aircraft and r and s are their respective derivatives.

The A matrices for these models, which are necessary for Pitch Paper Pilot, are shown on the following pages. Figure 8 shows the ninth order A matrix and Figure 9 shows the thirteenth order A matrix.

Optimization Results

The SAS gains were first optimized for the ninth order model, with no structural bending considered for fifteen flight conditions. Table VI shows the results. The table shows the minimum predicted rating, the augmentation system gains that produced it, and the calculated three-sigma value of actuator rate required. Note that

$$\begin{bmatrix}
 0 & 0 & 0 & 0 & 0 & 0 & 0 & 0 & 0 & 0 & 0 & 0 & 0 \\
 0 & M_q & 0 & M_w & M_{se} & 0 & 0 & 0 & 0 & 0 & 0 & 0 & 0 \\
 0 & A & -\omega_f & B & C & 0 & 0 & 0 & 0 & 0 & 0 & 0 & 0 \\
 0 & U_0 & 0 & Z_w & Z'_{se} & 0 & 0 & 0 & 0 & 0 & 0 & 0 & 0 \\
 0 & 0 & -\frac{1}{T_e} & 0 & -\frac{1}{T_e}(1+K_g) & \frac{1}{T_e} & -\frac{1}{T_e T_f} & -\frac{K_p T_f}{T_e T_f} & \frac{1}{T_e} & 0 & 0 & 0 & 0 \\
 0 & 0 & 0 & 0 & 0 & -\frac{2}{T} & \frac{4}{T T_f} & \frac{4 K_p T_f}{T T_f} & 0 & 0 & 0 & 0 & 0 \\
 -K_p & -K_p T_f & 0 & 0 & 0 & 0 & -\frac{1}{T_f} & K_p(1-\frac{T_f}{T}) & 0 & 0 & 0 & 0 & 0 \\
 0 & 0 & 0 & 0 & 0 & 0 & 0 & -\omega_b & 0 & 0 & 0 & 0 & 0 \\
 0 & 0 & 0 & 0 & 0 & 0 & 0 & 0 & 0 & 0 & 0 & 0 & -\omega_r
 \end{bmatrix}$$

$A = \omega_f(K_q \cdot \frac{K_n}{g} L_z M_u)$ $B = \omega_f \frac{K_n}{g} (-Z_w + L_z M_u)$ $C = \omega_f \frac{K_n}{g} [-Z'_e + L_z M_{se} - 4Z_e(\theta_{n_1} \theta_{n_2})]$

Figure 8. "A" Matrix without Bending Modes

$$\begin{array}{c}
 \left[\begin{array}{ccccccccccccccccccccccccccccc}
 0 & 1. & 0 & 0 & 0 & 0 & 0 & 0 & 0 & 0 & 0 & 0 & 0 & 0 & 0 & 0 & 0 & 0 & 0 & 0 & 0 \\
 0 & M_a & 0 & 0 & 0 & 0 & 0 & 0 & 0 & 0 & 0 & 0 & 0 & 0 & 0 & 0 & 0 & 0 & 0 & 0 & 0 \\
 0 & A & -\omega_f & B & C & 0 & 0 & 0 & 0 & 0 & 0 & 0 & 0 & 0 & 0 & 0 & 0 & 0 & 0 & F & G \\
 0 & U_0 & 0 & Z_w & Z'_{se} & 0 & 0 & 0 & 0 & 0 & 0 & 0 & 0 & 0 & 0 & 0 & 0 & 0 & 0 & 0 & 0 \\
 0 & 0 & -\frac{1}{T_e} & 0 & -\frac{1}{T_e}(1+K_d) & \frac{1}{T_e} & -\frac{1}{T_e T_r} & -\frac{1}{T_e T_r} & -\frac{K_p T_r}{T_e T_r} & \frac{1}{T_e} & 0 & 0 & 0 & 0 & 0 & 0 & 0 & 0 & 0 & 0 & 0 \\
 0 & 0 & 0 & 0 & 0 & -\frac{2}{r} & -\frac{4}{r T_r} & -\frac{4}{r T_r} & \frac{4 K_p T_r}{r T_r} & 0 & 0 & 0 & 0 & 0 & 0 & 0 & 0 & 0 & 0 & 0 & 0 \\
 -K_p & -K_p T_L & 0 & 0 & 0 & 0 & -\frac{1}{T_r} & -\frac{1}{T_r} & K_p \left(1 - \frac{T_r}{T_e}\right) & 0 & 0 & 0 & 0 & 0 & 0 & 0 & 0 & 0 & 0 & 0 & 0 \\
 0 & 0 & 0 & 0 & 0 & 0 & 0 & 0 & -\omega_b & 0 & 0 & 0 & 0 & 0 & 0 & 0 & 0 & 0 & 0 & 0 & 0 \\
 0 & 0 & 0 & 0 & 0 & 0 & 0 & 0 & 0 & -\omega_r & 0 & 0 & 0 & 0 & 0 & 0 & 0 & 0 & 0 & 0 & 0 \\
 0 & 0 & 0 & 0 & 0 & 0 & 0 & 0 & 0 & 0 & 0 & 0 & 0 & 0 & 0 & 0 & 0 & 0 & 0 & 1. & 0 \\
 0 & 1. \\
 0 & 0 & 0 & 0 & 0 & -4U_Z Z_{se} & 0 & 0 & 0 & 0 & 0 & 0 & 0 & 0 & 0 & -900 & 0 & 0 & -0.06 & 0 & 0 \\
 0 & 0 & 0 & 0 & 0 & -4U_0 Z_{se} & 0 & 0 & 0 & 0 & 0 & 0 & 0 & 0 & 0 & 0 & 0 & -2500 & 0 & 0 & -1.
 \end{array} \right]
 \end{array}$$

Figure 9. "A" Matrix with Bending Modes

TABLE VI. OPTIMUM GAG PARAMETERS, ACTUATOR RATE, AND PREDICTED RATING USING THE NINTH ORDER MODEL.

Flight Condition	K_q (sec)	K_n (rad/g)	K_d	Actuator Rate (rad/sec)	Rating
1	-0.24	-0.0014	-0.63	0.499	2.900
2	-0.17	-0.0002	-0.20	0.493	2.597
3	-0.09	-0.0001	0.09	0.499	2.510
4	-0.04	0.0001	-0.38	0.499	2.447
5	-0.04	0.0000	-0.48	0.499	2.452
6	-0.04	0.0001	-0.34	0.499	2.325
7	-0.07	0.0002	-0.54	0.495	2.184
8	-0.08	0.0002	-0.67	0.499	2.224
9	-0.06	0	-0.49	0.497	3.263
10	-0.09	0.0000	-0.59	0.487	2.916
11	-0.11	0.0004	-0.74	0.498	2.415
12	-0.15	0.0006	-0.77	0.499	2.620
13	-0.17	0.0007	-0.86	0.499	3.972
15	-0.20	0.0004	-0.69	0.499	2.808
16	-0.04	0.0017	-0.17	0.499	3.474

TABLE VII. ACTUATOR RATE AND PREDICTED RATING USING
THE THIRTEENTH ORDER MODEL WITH SAS PARAMETERS
FOUND IN THE NINTH ORDER OPTIMIZATION.

Flight Condition	Actuator Rate (rad/sec)	Predicted Rating
1	.502	2.900
2	.501	2.590
3	.500	2.511
4	.500	2.448
5	.501	2.450
6	.500	2.328
7	.499	2.184
8	.502	2.222
9	.501	3.262
10	.489	2.925
11	.500	2.412
12	.503	2.615
13	.501	3.975
15	.502	2.803
16	.502	3.475

though $\dot{\theta}$ is less than 0.3 rad/sec, as required, it is barely within limits for all flight conditions.

Next, the thirteenth order system was run without SAS optimization, using the optimal feedback gains from the ninth order results. As can be seen from the results, tabulated in Table VII, both predicted ratings and actuator rates were closely comparable for both models, though actuator rate limitations were exceeded for some cases. Apparently, the bending modes have little effect on the design in these cases.

As a further test, selected flight conditions with varied Mach number and dynamic pressures, were fully optimized with the thirteenth order model to see how the optimal SAS gains were changed. Table VIII shows the results of this test. Again, only negligible variation from the ninth order results was observed.

Table VIII. Optimum Parameters for Selected Flight Conditions with the Thirteenth Order Model.

Flight Condition	K_1 (sec^2)	K_2 (rad/g)	K	Actuator Rate (rad/sec)	Rating
1	-0.24	-0.0014	-0.62	0.499	2.901
7	-0.07	0.0001	-0.54	0.499	2.184
9	-0.06	0.0000	-0.49	0.483	3.119
10	-0.09	0.0000	-0.59	0.499	2.925

For the JACC Design Challenge, addition of the bending modes made little difference. Ninth order results could be used for all conditions. This has an extra advantage, since much less computer time was required for ninth order optimization.

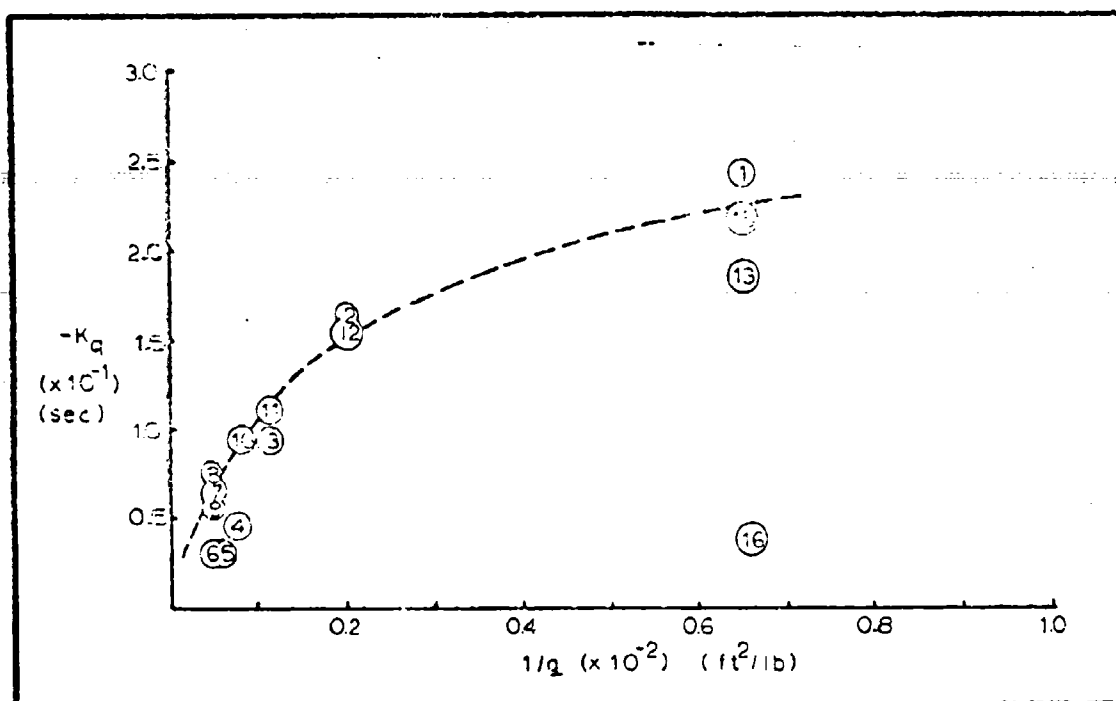
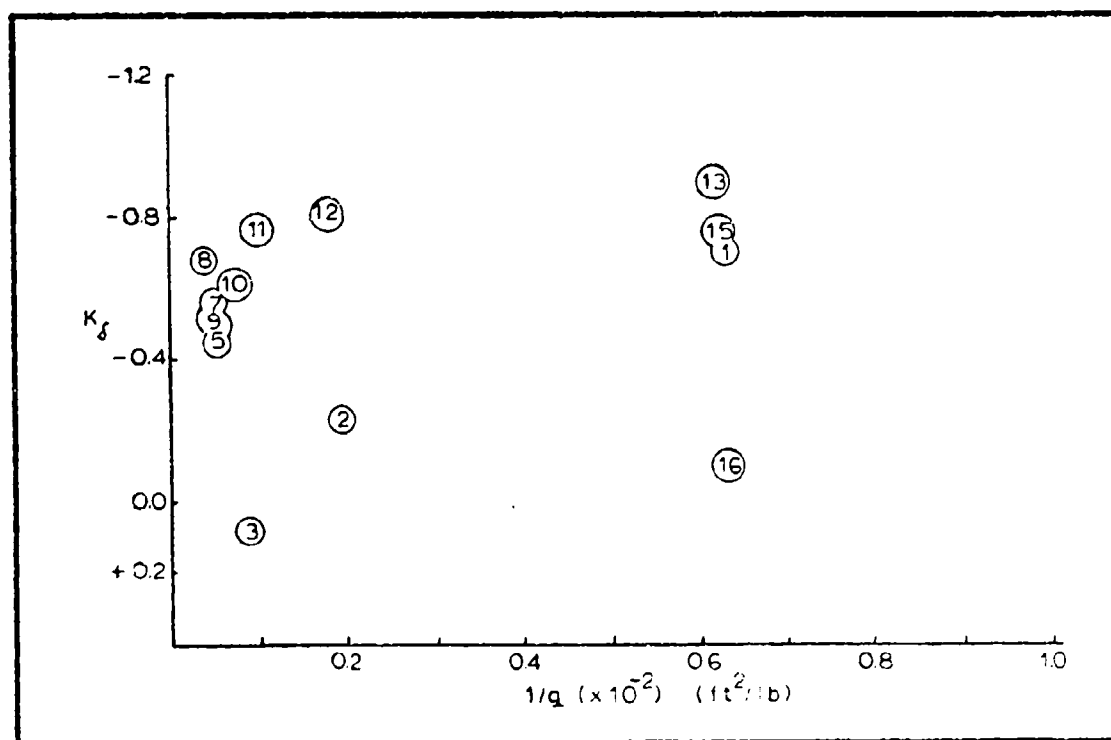
Gain Scheduling

In his study of a variable stability T-33, Hollis found a simple relationship between $1/q$ and the SAS feedback gains (3:33-38). This allowed the gains to be scheduled for the flight conditions, in relation to dynamic pressure.

The JACC Design Challenge optimization results showed a similar correlation between $1/q$ and pitch rate feedback gain. This is shown in Figure 10. Note that the gains are all grouped along a curve, with the exception of Flight Condition 16. No reason was found for this single variation.

No simple dependency could be found for elevator deflection feedback gain, K_{δ} . Figure 11 shows a graph of K_{δ} versus $1/q$.

Normal acceleration feedback gain was so close to zero in all cases that it would probably be considered zero for scheduling purposes.

Figure 10. K_q vs. $1/q$ for Optimal SAS.Figure 11. K_s vs. $1/q$ for Optimal SAS.

Addition of Pre-Filter

Analog simulation of the Design Challenge aircraft and SSS, as presented in Chapter V, revealed that a pre-filter on the pilot's input to the aircraft was needed to meet the design criteria. Without the pre-filter, an undesirable negative spike was present in the initial normal acceleration and acceleration rate which exceeded the envelopes defined in Chapter III. The pre-filter significantly improved this response for most flight conditions.

Adding the pre-filter produced a new system model of fourteenth order. Since the pre-filter was not in the original system model, it was reasonable to expect that the new model would have some effect on the predicted ratings from Paper Pilot.

The pre-filter is on the \dot{y}_p signal from the pilot model to the actuator (see Figure 7). Thus, the model is modified as shown in Figure 12.

The break frequency, ω_p , used here was 5 rad/sec. The new state equations for this fourteenth order mode are fully developed in Appendix D.

Table IX shows the results from Paper Pilot studies with the new state equations. The feedback gains from the

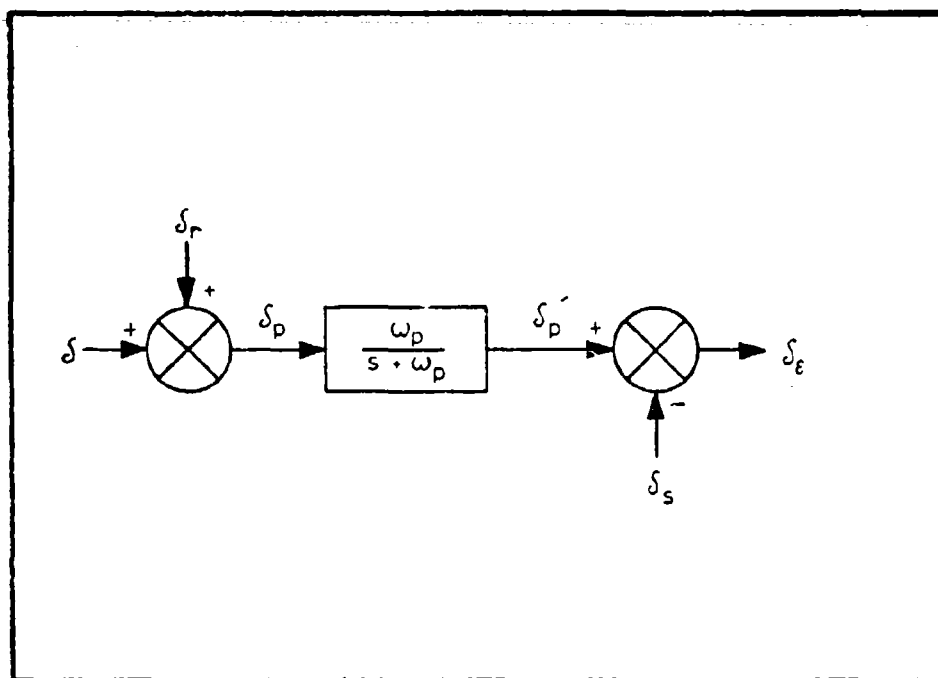


Figure 12. Pre-Filter.

TABLE IX. ACTUATOR RATE AND PREDICTED RATING FOR
MODEL WITH PRE-FILTER USING SAS PARAMETERS FROM
THE NINTH ORDER OPTIMIZATION.

Flight Condition	Actuator Rate (rad/sec)	Predicted ^a Rating
1	.224	2.186
2	.151	1.860
3	.104	1.748
4	.181	1.652
5	.201	1.601
6	.187	1.611
7	.210	1.603
8	.316	1.723
9		2 ^b
10	.190	1.775
11	.199	1.849
12	.192	2.031
13	.217	3.074
15	.181	2.194
16	.093	2.705

a. Drop in ratings from the original ninth order values ranged from 0.5 to 1.0 ratings with most values around 0.8 ratings.

b. Flight condition 9 would not converge for this situation (T_L near zero), so no actuator rate was calculated. The rating was estimated from the point of closest convergence (gradient of 1.6).

ninth order SAS optimization were used to find new predicted pilot ratings and actuator rates. As shown in Table IX, the addition of the pre-filter produced a substantial change in both predicted rating and actuator rate. Note that all ratings were lowered by about the same amount.

With both the rating and actuator rate lowered, it was expected that a SAS gain optimization for any flight condition would further lower predicted pilot ratings while raising the actuator rate close to the limit. Flight condition 1 was checked to test this hypothesis. As shown in Table X below, the expected result occurred.

TABLE X. COMPARISON OF PARAMETERS FOR FLIGHT CONDITION 1.

	K_d (sec)	K_n (rad/g)	K_f	Actuator Rate (rad/sec)	Rating
9th Order Optimum	-0.24	-0.0014	-0.63	0.499	2.900
13th Order Optimum	-0.24	-0.0014	-0.62	0.499	2.901
14th Order Optimum w/ 9th Order Parameters	-0.24	-0.0014	-0.63	0.224	2.186
14th Order Optimum	-0.44	-0.0029	-0.61	0.499	1.866

Although some studies were done with the system including the pre-filter, a great deal more work could be done in this area.

Conclusions

The SAS optimization procedure, including Pitch Paper Pilot, worked well for this system. In general, the procedure works well for systems of a reasonable order and with few feedback states. Increasing the order of the system or the number of feedback parameters requires causes a large increase in computer time. For instance, increasing the order from ninth to thirteenth order approximately doubled the required computer time. The Air Force Flight Dynamics Laboratory has improved some of the search routines within Paper Pilot to reduce time requirements, which should help to alleviate this problem. As stated earlier, the bending modes did not significantly influence the SAS design in this case.

V. Simulation

Procedure - Commanded δ_e Response

The Design Challenge aircraft and the SAS were simulated on an EAI Pace analog computer. For comparison purposes, and to check the computer patching, the system was first run open loop, that is, without the stability augmentation system. Then, the feedback loops were closed. The input for both cases was a commanded step elevator deflection. The plots are presented in Appendix C.

Throughout the simulation, only the mean values of the stability derivatives and flexure mode parameters were used. The additive white noise terms in the equations of the states perturbed by the flexure were dropped. It was assumed that the analog computer generated enough inner noise to compensate for the elimination of these terms.

Flight Conditions 1, 3, 5, 9 and 13 are presented here as a cross-section of the possible combinations of Mach number and dynamic pressure. Table XI gives a comparison of these values for the five flight conditions.

JACC Design Challenge Response Envelopes

Before examining the closed loop aircraft responses, several points should be made about the JACC Design Challenge normal acceleration response envelopes. Their shapes appear to be contrived limits on more conventional parameters such

Table XI. Comparison of Flight Conditions

Flight Condition	Dynamic Pressure	Mach Number
1	low	low
3	medium	medium
5	high	medium
9	high	high
13	low	high

as rise time, settling time, peak overshoot and under-shoot. It is difficult to say whether or not these envelopes actually represent good handling qualities in the opinion of a pilot. Consequently, the Design Challenge envelopes may not be good criteria for evaluating the response of an aircraft with a SAS design based on pilot rating.

In addition, the normalizing factor, τ , was a discrete function of dynamic pressure. Depending on how it was arrived at, this non-linearity could over-restrict responses for either the extreme values of q or for the middle values. In any case, τ as a continuous function of q would have perhaps been a better normalizing constant.

Regardless, the Design Challenge response envelopes were used as the criteria to judge the normal accelera-

tion response of the augmented aircraft. They did provide a quick "eyeball" assessment of the final closed loop response.

Normal Acceleration Response

All five flight conditions had a response with a large negative normal acceleration spike at $t = 0+$. It was especially noticeable in Flight Conditions 1, 9, and 13. The spike appeared, with the exception of Flight Condition 9, in cases where the g was low, which is reasonable if one considers the aircraft in such an environment. In order to achieve a quick rise time at low dynamic pressure, the control action of an elevator deflection translates the aircraft vertically downward before rotation occurs. With a high g the elevator has greater pitch control effectiveness, thus the aircraft does not experience so great a negative n_z . Flight Condition nine is affected more by other factors and will be discussed later.

Pre-Filter

To deal with the negative normal acceleration spike problem, a pre-filter was added to shape the pilot's commanded input. The corresponding equations are presented in Chapter 4. The filter was not used initially in the

optimization routine since the fixed-form SAS was chosen to be solely the feedback system in Figure 7. However, the pre-filter was added after the simulation results showed an undesirable spike in the output. Table IX shows that the change in pilot rating was significant after the addition of the filter. Since no extensive SAS optimization was performed with the pre-filter in the system, it is impossible to say just what its effect would be on the final closed loop response. Probably one of two possibilities would result. Either the optimization and resulting feedback gains would bring a negative spike back into the response, or the filtered input would be sufficient to yield a final response without the high frequency spike. However, this study was concerned only with augmenting the aircraft with a feedback SAS, and the filter was added merely to check its effect on the negative spike, regardless of its effect on the rest of the response. It was concluded that the original SAS design was still valid in its "optional" sense.

The pre-filter used was a first order lag. Break frequencies of both 2 and 5 radians per second were tried for each flight condition.

The addition of the filter brought the responses closer to the prescribed envelopes, but in general the negative spike was still large enough to fall outside of

the envelope. The effect of the filter depended on the "frequency" of the spike. A short narrow spike, such as on flight condition 5, was effectively removed by the filter, while a long, wide spike, such as on flight condition 13, remained with the filter in operation. For the most part, the filter with a break frequency of 2 was too restrictive, lowering rise times below acceptable limits. Perhaps a new optimization with this filter employed would yield better performance characteristics.

High Frequency, Low Damping

The closed loop response for flight condition 9 falls outside the Design Challenge envelopes. The reason for the failure of the Paper Pilot in this case seems to be the same problem as discussed in Chapter II. The Paper Pilot does not accurately reflect pilot opinion in the case of an aircraft with a high natural frequency and low damping. Table XII shows the open loop short period parameters for the simulated flight conditions. The final column, "Improvement in Closed Loop Response", is a judge of how much the SAS improved any deficiencies in the open loop response. Flight condition 9, with a ζ of 0.109 and ω_n of 5.51, falls into the region where the Paper Pilot had previously failed. It must be concluded, therefore, that the addition of remnant, discussed in Chapter II, did not completely solve the problem. Further

Table XII. Short Period Parameters
and Closed Loop Response Quality

Flight Condition	ω_{nsp}	ζ_{sp}	Pilot Rating	Improvement in Closed Loop Response
1	1.26	0.238	2.90	Very Good
3	4.30	0.386	2.51	Good
5	8.08	0.337	2.45	Fair
9	5.51	0.109	3.27	Poor
13	1.74	0.035	3.97	Very Good

support of this conclusion can be found in Table XII. Flight condition 13, with an equally poor open loop response, yet a lower frequency, was improved significantly when the SAS was added. The final pilot rating was 3.97. Flight condition 9, received a better pilot rating, 3.27, yet the closed loop response was considered very poor.

Flight condition 5 also fell into this high frequency, low damping region. While the final closed loop response was not bad, the degree of improvement over the open loop response was slight, indicating once again the problem with Paper Pilot.

A possible cure for this problem would be the addition of a normal acceleration term or pitch rate term (which is related to normal acceleration) in the cost function used

term be added to the Paper Pilot rating expression to correct this problem.

Although a good design procedure, Paper Pilot proved to be very costly in computer time. The Air Force Flight Dynamics Laboratory has recently improved search procedures to lower the computer time. Also, reducing the state vector of the entire system by approximations significantly reduces the required time. In this study it was found that ignoring the two second order bending modes of the Design Challenge aircraft made little change in the SAS design yet greatly improved computer time.

Recommendations for Future Study

In light of various problems and insights encountered during the course of this study, the following suggestions are offered for future work using Paper Pilot:

1. Incorporate a pitch rate or normal acceleration term into the pilot rating expression in Pitch Paper Pilot.
2. Optimize pilot ratings with respect to pilot lag as well as lead and gain, to study effects on high frequency, low damping cases.
3. Find optimal SAS gains for the JACC Design Challenge with a pre-filter included in the system.

Applying some of these refinements, Pitch Paper Pilot could prove to be a very useful tool in SAS design.

ft/sec, which is a rather small vertical wind gust.

It is not unreasonable to find that the aircraft does

not respond to this small disturbance.

Comparisons

The JACC Design Challenge was studied earlier by Sherrard, Ward and Paul. Sherrard used optimal control techniques, Ward used classical control techniques and Paul used self-adaptive control techniques. Comparing the simulation results of those studies with the results presented in Appendix C illustrates the success of Paper Pilot. Paper Pilot optimization gave better compliance with the Design Challenge response envelopes than flight conditions 3 and 5 in Sherrard, 1 and 3 in Ward, and 1, 3 and 13 in Paul. In those flight conditions, Paper Pilot had better rise times or damping in the normal acceleration responses.

VI. Conclusions

Paper Pilot offers a viable method of SAS parameter optimization for SAS design. Selecting SAS gains that give the minimum pilot rating for a particular aircraft configuration results in SAS parameters that are pilot rating optimal. In this study, this method often resulted in a closed loop response that was as good as or better than the response from designs by classical or modern control techniques.

Initially, Pitch Paper Pilot was modified to include terms for pilot remnant and lag in the pilot model. This was to improve the accuracy of the predicted pilot ratings for flight conditions with a high short period natural frequency and low damping. This was not the total answer, as some inaccuracy still existed after the modifications.

Paper Pilot was next used to select SAS gains for the JACC Design Challenge aircraft. An undesirable negative normal acceleration spike appeared in the analog simulation of the closed loop aircraft. Adding a pre-filter to shape the pilot's commanded input improved this aspect, but complete SAS parameter optimization with the pre-filter included was left to future studies. The problem with high frequency and low damping conditions appeared again, and it was suggested that a pitch rate

term be added to the Paper Pilot rating expression to correct this problem.

Although a good design procedure, Paper Pilot proved to be very costly in computer time. The Air Force Flight Dynamics Laboratory has recently improved search procedures to lower the computer time. Also, reducing the state vector of the entire system by approximations significantly reduces the required time. In this study it was found that ignoring the two second order bending modes of the Design Challenge aircraft made little change in the SAS design yet greatly improved computer time.

Recommendations for Future Study

In light of various problems and insights encountered during the course of this study, the following suggestions are offered for future work using Paper Pilot:

1. Incorporate a pitch rate or normal acceleration term into the pilot rating expression in Pitch Paper Pilot.
2. Optimize pilot ratings with respect to pilot lag as well as lead and gain, to study effects on high frequency, low damping cases.
3. Find optimal SAS gains for the JACC Design Challenge with a pre-filter included in the system.

Applying some of these refinements, Pitch Paper Pilot could prove to be a very useful tool in SAS design.

Bibliography

1. Anderson, R. O., Connors, A. J., and Dillow, J. D. Paper Pilot Roll-Pitch. AFFDL/PGC-TM-70-1, November, 1970.
2. Dillow, James D. The Paper Pilot-- A Digital Computer Program to Predict Pilot Rating for the Hover Task. AFFDL-PR-70-40, March 1971.
3. Hollis, Teddy L. Optimal Selection of Stability Augmentation System Parameters to Reduce Pilot Rating for the Hover Task. AFIT Thesis GGC/EE/71-10. Air Force Institute of Technology, Wright-Patterson AFB, Ohio, June 1971.
4. McRuer, Duane T. and Jex, Henry R. A Review of Quasi-Linear Pilot Models. Transactions on Human Factors in Electronics, IEEE, Vol. 8, September 1967.
5. Naylor, Flynn. Predicting Roll Task Flying Qualities with Paper Pilot. AFIT Thesis GGC/EA/73-1. Air Force Institute of Technology, Wright-Patterson AFB, Ohio, September 1972.
6. Paul, Richard R. Applications of Self-Adaptive Control System Techniques in the Design of a Normal Acceleration Control System for a High Performance Supersonic Aircraft. AFIT Thesis GGC/EE/71-7. Air Force Institute of Technology, Wright-Patterson AFB, Ohio, June 1971.
7. Rediess, Herman A. and Taylor, Lawrence W. A Flight Control System Design Problem for the Design Challenge to the 1970 Joint Automatic Control Conference. Released at the 1970 JACC, Atlanta, Georgia, June 1970.
8. Sherrard, Ancel R. An Investigation of the Applicability of Linear Optimal Control Theory to Aircraft Control System Design. AFIT Thesis GGC/EE/71-22. Air Force Institute of Technology, Wright-Patterson AFB, Ohio, March 1971.
9. Ward, Ralph R. A Classical Design Approach to a Normal Acceleration Stability Augmentation System for High-Performance Aerospace Vehicle. AFIT Thesis GGC/EE/71-25. Air Force Institute of Technology, Wright-Patterson AFB, Ohio, June 1971.



GGC/EE/73-3

10. Zuckerman, Meyer D. Investigation of Glide-Slope Information Rate Requirements for a Low-Visibility Aircraft Landing. AFIT Thesis GE/EE/71-30. Air Force Institute of Technology, Wright-Patterson AFB, Ohio, March 1971.

Appendix A

System Equations in State Variable Form

Aircraft Equations of Motion

The linearized longitudinal short period equations are (7:3)

$$\dot{\theta} = q \quad (22)$$

$$\dot{q} = M_{\alpha}\alpha + M_q q + M_{\dot{\delta}_e} \dot{\delta}_e + M_{\alpha} \frac{w}{U_0} \quad (23)$$

$$\dot{\alpha} = Z_{\alpha}\alpha + q + Z_{\dot{\delta}_e} \dot{\delta}_e + Z_{\alpha} \frac{w}{U_0} \quad (24)$$

Since normal acceleration is used as a feedback state in place of angle or attack, an equation for normal acceleration is needed. This is

$$n_z = \frac{U_0}{g} (q - \dot{\alpha}) \quad (25)$$

Substituting equation (24) into equation (25) and ignoring the wind gust terms yields

$$\begin{aligned} n_z &= \frac{U_0}{g} (-Z_{\alpha}\alpha - Z_{\dot{\delta}_e} \dot{\delta}_e) \\ &= \frac{U_0}{g} Z_{\alpha}\alpha - \frac{U_0}{g} Z_{\dot{\delta}_e} \dot{\delta}_e \end{aligned} \quad (26)$$

Using the fact that $w = U_0\alpha$ and letting $M_w = \frac{M_{\alpha}}{U_0}$, $Z_w = Z_{\alpha}$, $Z_{\dot{\delta}_e}' = U_0 Z_{\dot{\delta}_e}$ equations (23), (24) and (26) can be rewritten

$$\dot{q} = M_w w + M_q q + M_{\dot{\delta}_e} \dot{\delta}_e \quad (27)$$

$$\dot{w} = Z_w w + U_0 q + Z_{\dot{\delta}_e}' \dot{\delta}_e \quad (28)$$

$$n_z = -\frac{Z_w}{g} w - \frac{Z_{\dot{\delta}_e}'}{g} \dot{\delta}_e \quad (29)$$

The final short period equations are (22), (27) and (28).

Servoactuator

The elevator servoactuator is represented by a first order time lag, with a time constant of 0.05 seconds.

This is shown in Figure 13.

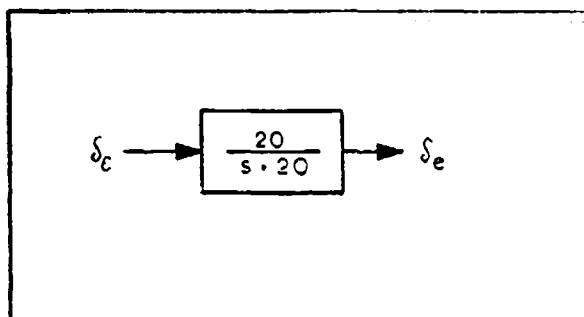


Figure 13. Servoactuator Model

The equation resulting from this is

$$\dot{\delta}_e = -20\delta_e + 20\delta_c \quad (30)$$

Stability Augmentation System

The Stability Augmentation System (SAS) used is shown in Figure 7. Structural flexibility was introduced into the system through the pitch rate and normal acceleration sensors. The sensors are rigidly fixed to the aircraft and cannot be moved to a "node" to remove the effects of body bending. However, as shown in Figure 7, the sensor outputs are filtered before fed back. The sensor outputs also contain additive white noise.

For this aircraft, the break frequency of the filter was chosen as 3. This was the value arrived at by Sherrard, and represented a good choice of maximum attenuation of body bending effects with minimum attenuation of the rigid body dynamics (8:28).

From the design challenge the indicated pitch rate and indicated normal acceleration measurement equations are

$$q_i = q - \lambda_{\theta_1} \dot{u}_1 - \lambda_{\theta_2} \dot{u}_2 + q_n \quad (31)$$

$$n_{zi} = n_z + \frac{1}{g} (L_z \dot{q} + \phi_{n1} \ddot{u}_1 + \phi_{n2} \ddot{u}_2) + n_{zn} \quad (32)$$

The first order filter yields the two expressions

$$\dot{n}_{zf} = -\omega_f n_{zf} + \omega_f n_{zi} \quad (33)$$

$$\dot{q}_f = -\omega_f q_f + \omega_f q_i \quad (34)$$

The first and second body bending modes are represented by

$$\ddot{u}_1 + (2\zeta_1 \omega_1) \dot{u}_1 + (\omega_1)^2 u_1 = \psi \delta_e \quad (35)$$

$$\ddot{u}_2 + (2\zeta_2 \omega_2) \dot{u}_2 + (\omega_2)^2 u_2 = \psi \delta_e \quad (36)$$

Letting

$$\begin{aligned} r &= \dot{u}_1 \\ s &= \dot{u}_2 \end{aligned} \quad (37)$$

and substituting in the values of ζ , ω and ψ yield the body bending equations as used here

$$\dot{r} + .06r + 900 u_1 = -4U_0 Z \delta_e \quad (38)$$

$$\dot{s} + s + 2500 u_2 = -4U_0 Z \delta_e \quad (39)$$

The final SAS output is

$$J_s = K_s J_e + K_q q_f + K_n n_{zf} \quad (40)$$

Multiplying equation (34) by K_q , equation (33) by K_n , and combining

$$\begin{aligned} & K_q \dot{q}_f + K_n \dot{n}_{zf} \\ &= -\omega_f (K_q q_f + K_n n_{zf}) + \omega_f (K_q q_i + K_n n_{zi}) \end{aligned} \quad (41)$$

Now define a new state.

$$\beta \triangleq K_q q_f + K_n n_{zf} \quad (42)$$

Differentiating this and equating the result to (41)

$$\begin{aligned} \dot{\beta} &= K_q \dot{q}_f + K_n \dot{n}_{zf} \\ \dot{\beta} &= -\omega_f \beta + \omega_f K_q q_i + \omega_f K_n n_{zi} \end{aligned} \quad (43)$$

Substituting equations (27) and (29) into (32) yields

$$\begin{aligned} n_{zi} &= -g Z_w w - q Z_{J_e} J_e \\ &+ \frac{1}{g} (L_z M_w w + L_z M_q q + L_z M_{J_e} J_e) \\ &+ \frac{1}{g} (\phi_{n1} \dot{r} + \phi_{n2} \dot{s}) + n_{zn} \end{aligned} \quad (44)$$

Finally, after substituting equations (31) and (44) into equation (43), the final equation for β results

$$\begin{aligned} \dot{\beta} &= -\omega_f \beta \\ &+ \omega_f \left(K_q + \frac{K_n}{g} L_z M_q \right) q \\ &+ \omega_f \frac{K_n}{g} (-Z_w + L_z M_w) w \\ &+ \omega_f \frac{K_n}{g} [-Z_{J_e}' + L_z M_{J_e} - 4 Z_{J_e}' (\phi_{n1} + \phi_{n2})] J_e \end{aligned}$$

$$- \omega_f (K_q \lambda_{e_1} + 0.6 \frac{K_n}{g} \phi_{n_1})$$

$$- \omega_f (K_q \lambda_{e_2} + \frac{K_n}{g} \phi_{n_2})$$

$$- 900 \omega_f \frac{K_n}{g} \phi_{n_1} v_1$$

$$- 2500 \omega_f \frac{K_n}{g} \phi_{n_2} v_2$$

$$+ \omega_f K_q q_n + \omega_f K_n n z_n$$

(45)

Appendix B

State Equations from the Pilot Model

As shown in Figure 2, the pilot model responds to a pitch error through a lag and lead network and pure time delay, with remnant added at the output. The output of the pilot model, modified by the system feedback, is the command to the actuator.

Time Delay. For purposes of simplicity of calculation and modeling, the time delay is approximated by the Padé expansion, thus

$$e^{-\tau s} = \frac{\hat{s}}{\hat{s}'} = \frac{(s+0.5\tau)}{(s+0.5\tau)} \quad (46)$$

This can be re-written

$$\hat{s}' + \hat{s} = \frac{2}{\tau} (\hat{s}' - \hat{s}) \quad (47)$$

Define a new state

$$y_1 \triangleq \hat{s}' + \hat{s} \quad (48)$$

By substitution

$$y_1 = \frac{2}{\tau} (-y_1 + 2\hat{s}') \quad (49)$$

Lag-lead Network. Now, from the transfer function

$$\frac{\hat{s}'}{\theta_e} = \frac{K_p(T_L s + 1)}{(T_I s + 1)} \quad (50)$$

letting $\theta_e = \theta_c - \theta$ and $q = \dot{\theta}$

$$\hat{s}' T_I - K_p T_L \dot{\theta}_c = -\hat{s}' - K_p T_L q + K_p \theta_c - K_p \theta \quad (51)$$

Define a new state

$$y_2 = T_I \hat{s}' - K_p T_L \theta_c \quad (52)$$

By substitution

$$\dot{y}_2 = -\dot{s}' - K_p T_L q + K_p \theta_c - K_p \theta \quad (53)$$

From the equation for y_2

$$\dot{s}' = \frac{y_2}{T_1} + \frac{K_p T_L}{T_1} \theta_c \quad (54)$$

Pitch Command. From the system diagram, Figure 7, the commanded pitch, θ_c , is

$$\theta_c = \frac{\dot{s}}{s + \omega_b} \quad (55)$$

where \dot{s} is a zero-mean gaussian white noise. Therefore

$$\dot{\theta}_c = -\omega_b \theta_c + \dot{s} \quad (56)$$

Actuator Equation. Again from the system diagram, the actuator equation is

$$\dot{s}_e = -\frac{1}{T_e} s_e + \frac{1}{T_e} s_e \quad (57)$$

However, since, from the system diagram,

$$\dot{s}_e = \dot{s} - \dot{s}_s + \dot{s}_r = y_1 - \dot{s}' - \dot{s}_s + \dot{s}_r \quad (58)$$

and from Appendix A,

$$\dot{s}_s = K_s s_e + \beta \quad (59)$$

By substitution

$$\dot{s}_e = -\frac{1}{T_e} s_e - \frac{K_s}{T_e} s_e + \frac{1}{T_e} y_1 - \frac{1}{T_e} \dot{s}' - \frac{1}{T_e} \beta + \frac{1}{T_e} \dot{s}_r \quad (60)$$

Remnant. From the system diagram. Figure 7

$$\dot{s}_r = \frac{\dot{s}_r}{s + \omega_r} \quad (61)$$

which can be re-written

$$\dot{\zeta}_r = -\omega_r \zeta_r + \dot{\zeta}_r \quad (62)$$

System Equations. By proper substitution of the above results, the equations shown below are formed. When combined with the airframe and SAS equations from Appendix A, they form a complete set of system equations for this pilot-vehicle model.

$$\dot{y}_1 = \frac{2}{\tau}(-y_1 + \frac{2}{T_I} y_2 + \frac{2K_p T_L}{T_I} \theta_c) \quad (63)$$

$$\dot{y}_2 = -K_p T_L q - K_p \theta - \frac{1}{T_I} y_2 + K_p (1 - \frac{T_L}{T_I}) \theta_c \quad (64)$$

$$\dot{\theta}_c = -\omega_b \theta_c + \dot{\zeta} \quad (56)$$

$$\begin{aligned} \dot{\zeta} = & -\frac{1}{T_e}(1+K_f) \zeta_e + \frac{1}{T_e} y_1 - \frac{1}{T_e T_I} y_2 \\ & - \frac{1}{T_e T_I} K_p T_L \theta_c + \frac{1}{T_e} \zeta_r - \frac{1}{T_e} \beta \end{aligned} \quad (65)$$

$$\dot{\zeta}_r = -\omega_r \zeta_r + \dot{\zeta}_r \quad (62)$$

Appendix C

Simulation Results

The results of the simulation for flight conditions 1, 3, 5, 7 and 9 are shown here. The input is a command step pulse, whose magnitude is unimportant since the outputs are normalized. For each flight condition, the aircraft is first run open loop, that is, without a stabilization system. Then the loop is closed with the FAS with gains designated as optimal by the Paper Pilot Procedure. The last two plots for each flight condition include pre-filters between the pilot's commanded input and the aircraft. This pre-filter is a first order lag. It is first used with a break frequency of 5 radians per second, then reduced to 2 radians per second.

The final plot is that of the aircraft response to the specified vertical wind gust (2.821 ft/sec rms). All flight conditions here, both open and closed loop, showed zero response to the gust on the indicated scale. Therefore, only one flight condition is presented.

GGC/EE/73-3

Flight Condition 1

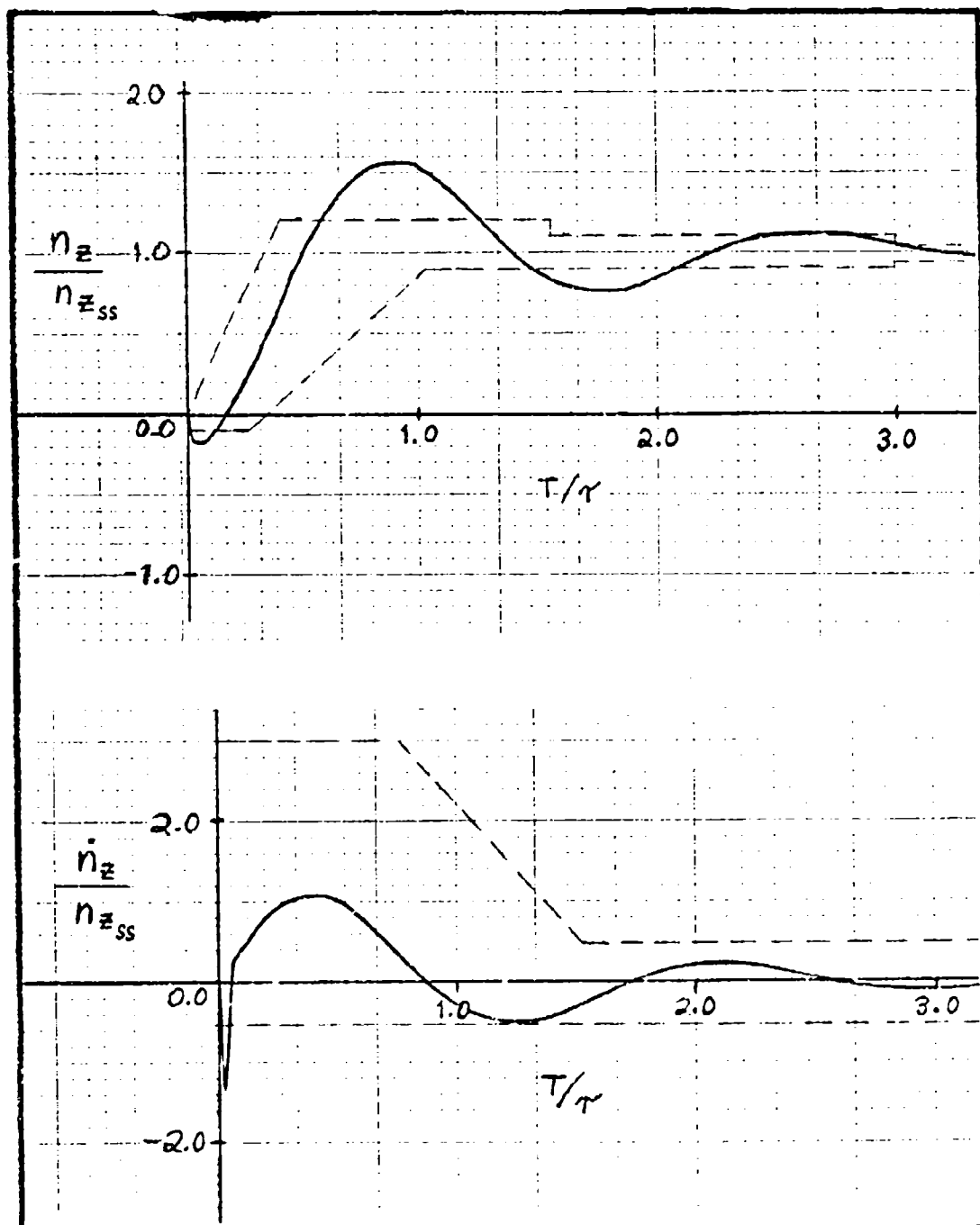


Figure 14. Op. 1000 Aircraft Response for Limit Condition 1.

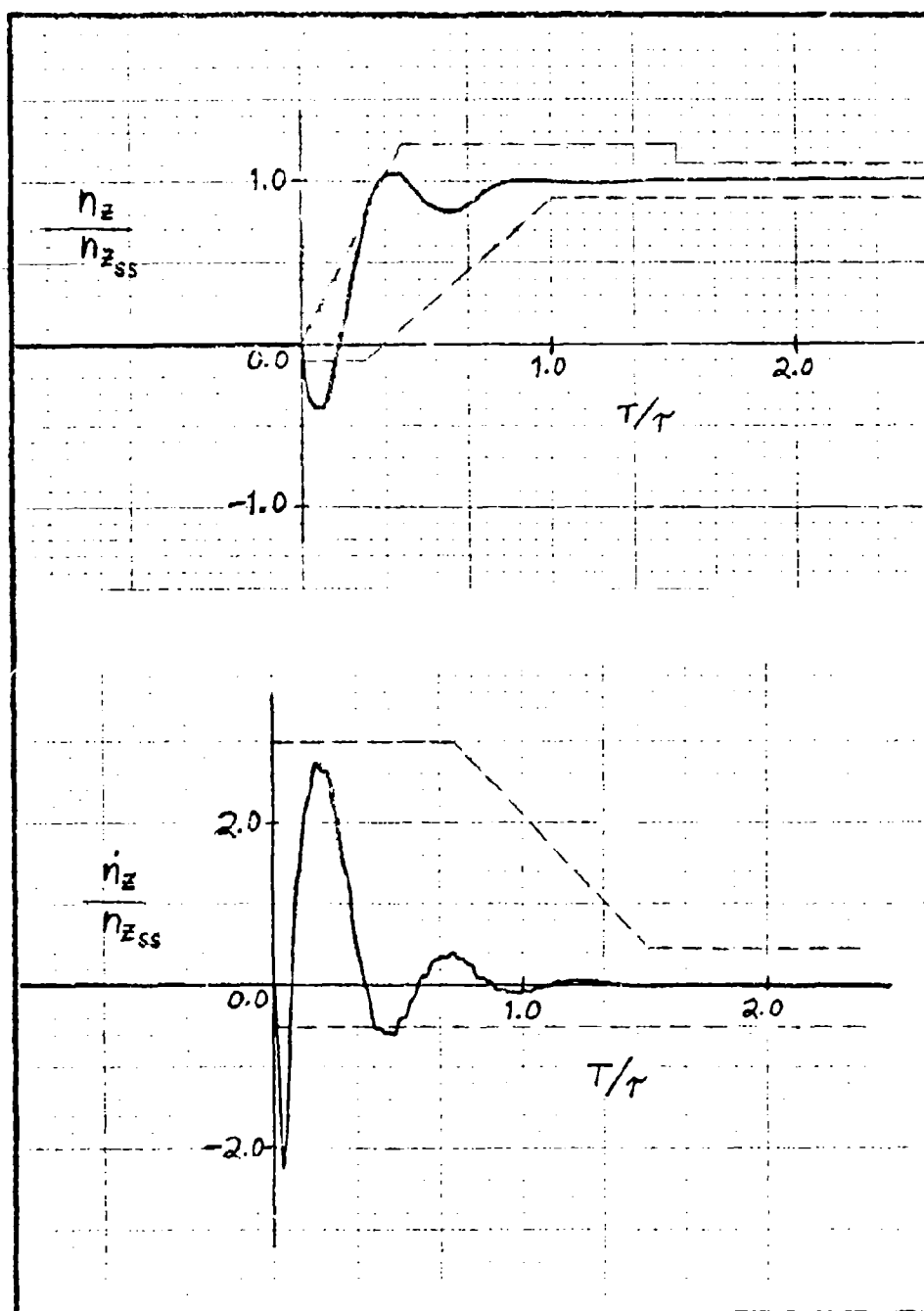


Figure 15. Closed loop Aircraft response for Condition 1.

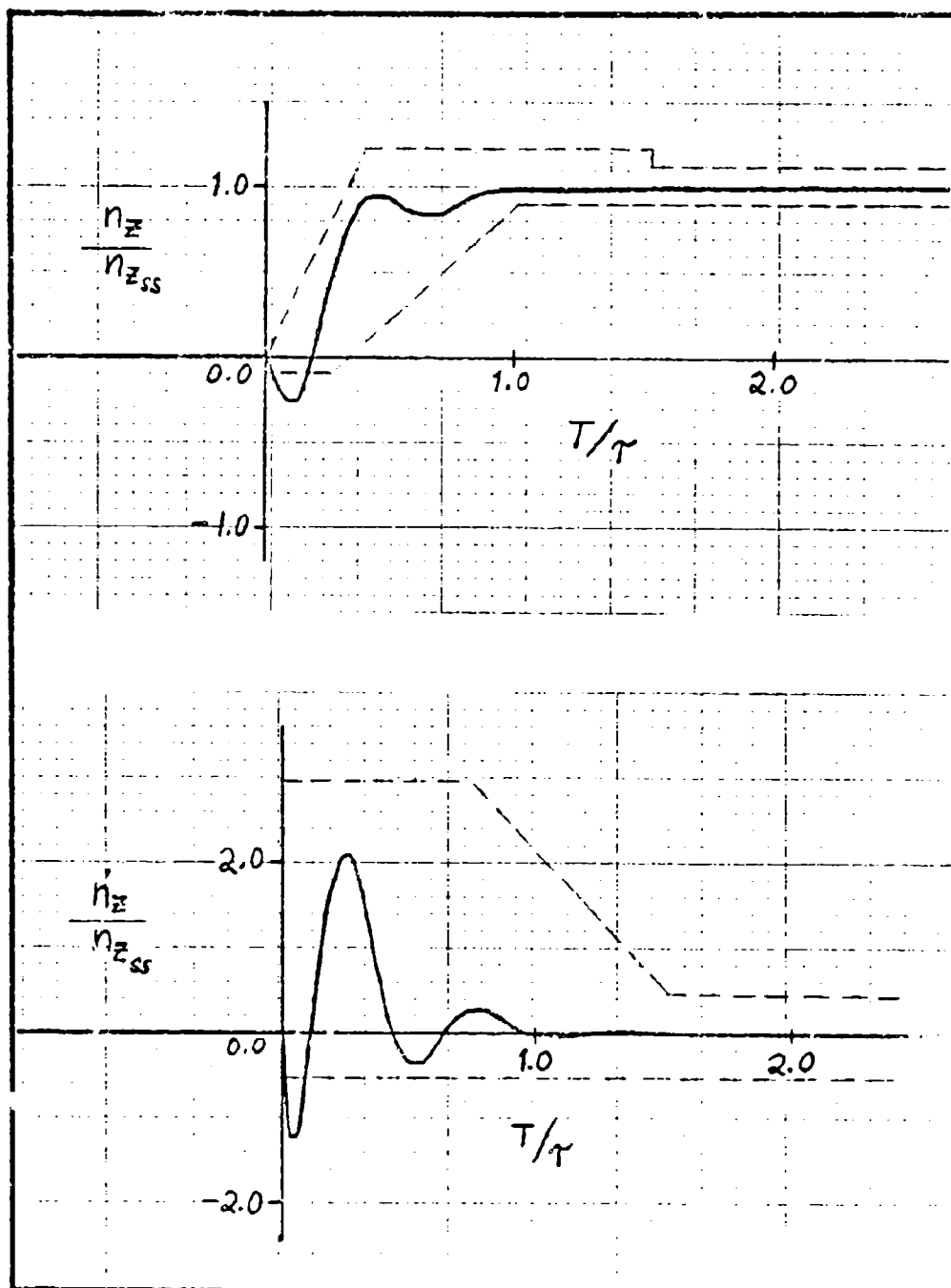


Figure 10. Closed loop aircraft response with pre-filter for flight condition 1; rear Frequency 5 rad/sec.

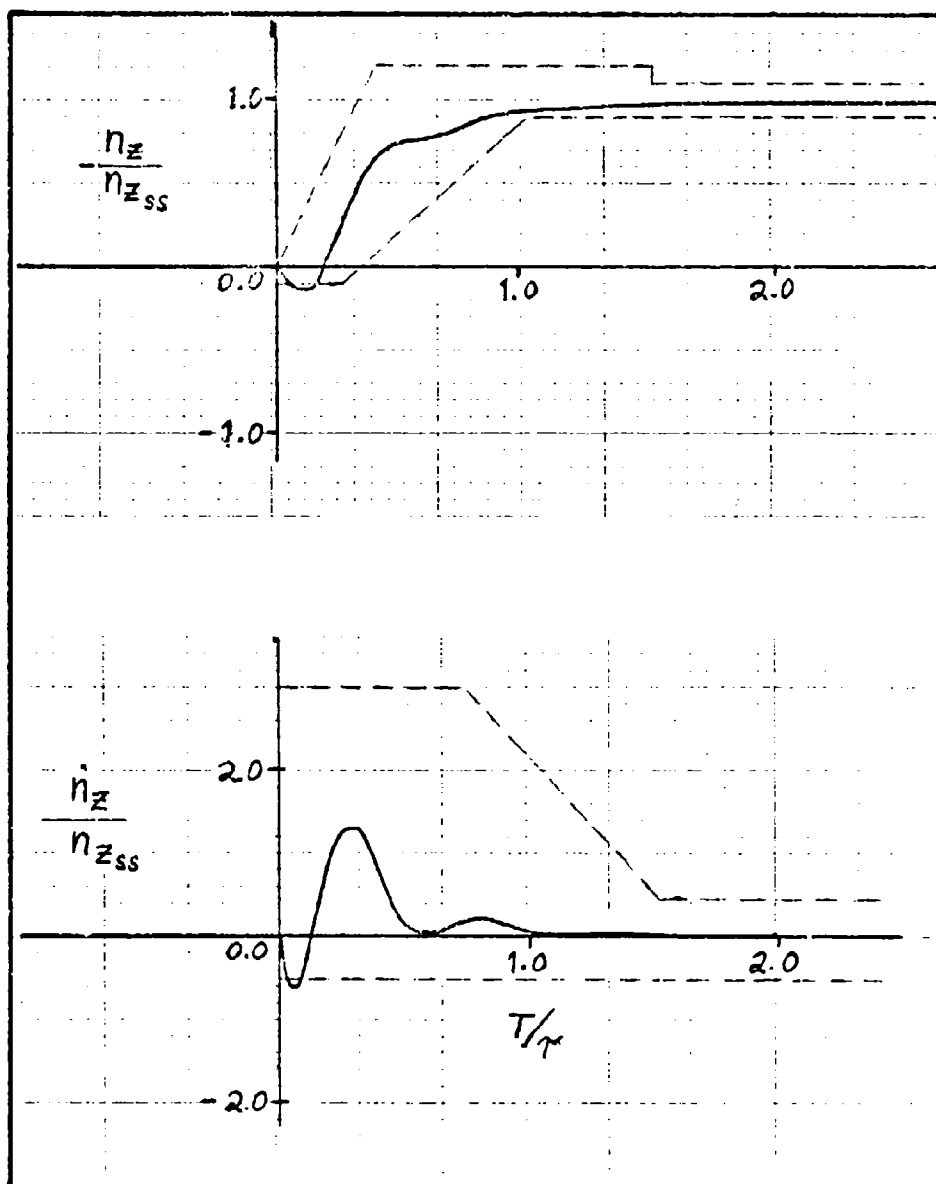


Figure 17. Closed Loop Aircraft Response with Pre-Filter for Flight Condition 1; break Frequency 2 rad/sec.

GGO/BE/73-3

Flight Condition 2

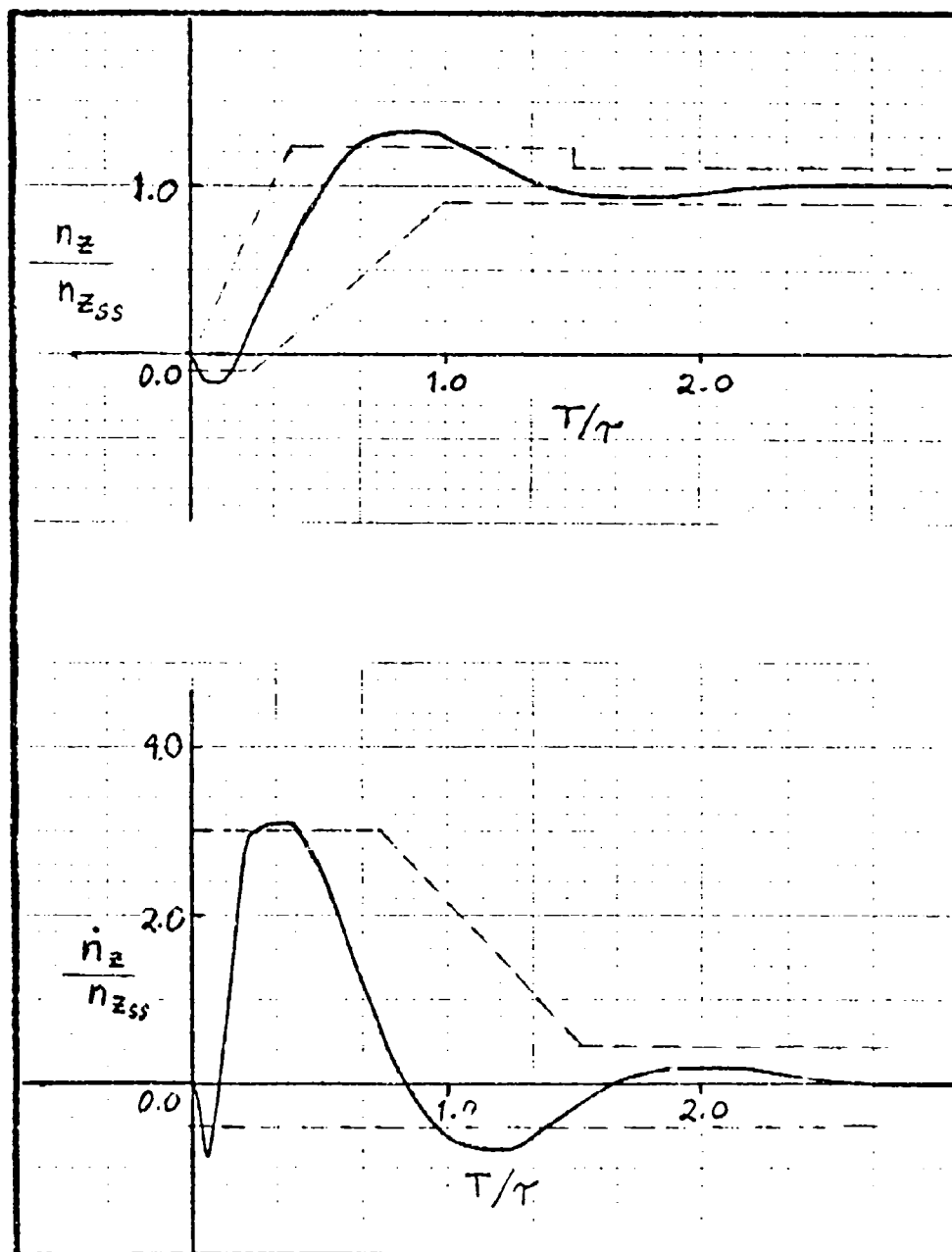


Figure 16. Open Loop Aircraft Response for Flight Condition 2.

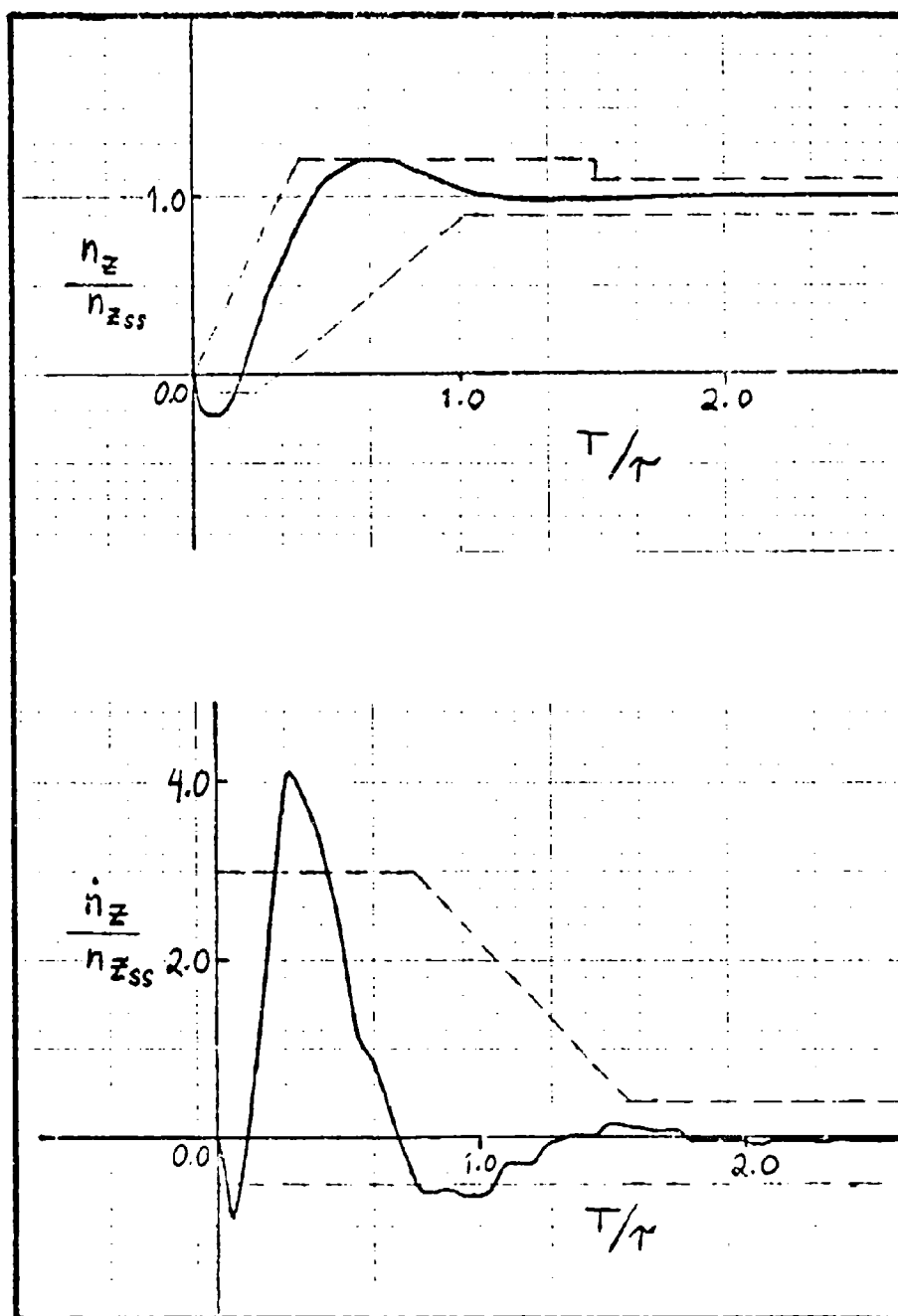


Figure 14. Cloned Ship Aircraft Control for Flight Condition 3.

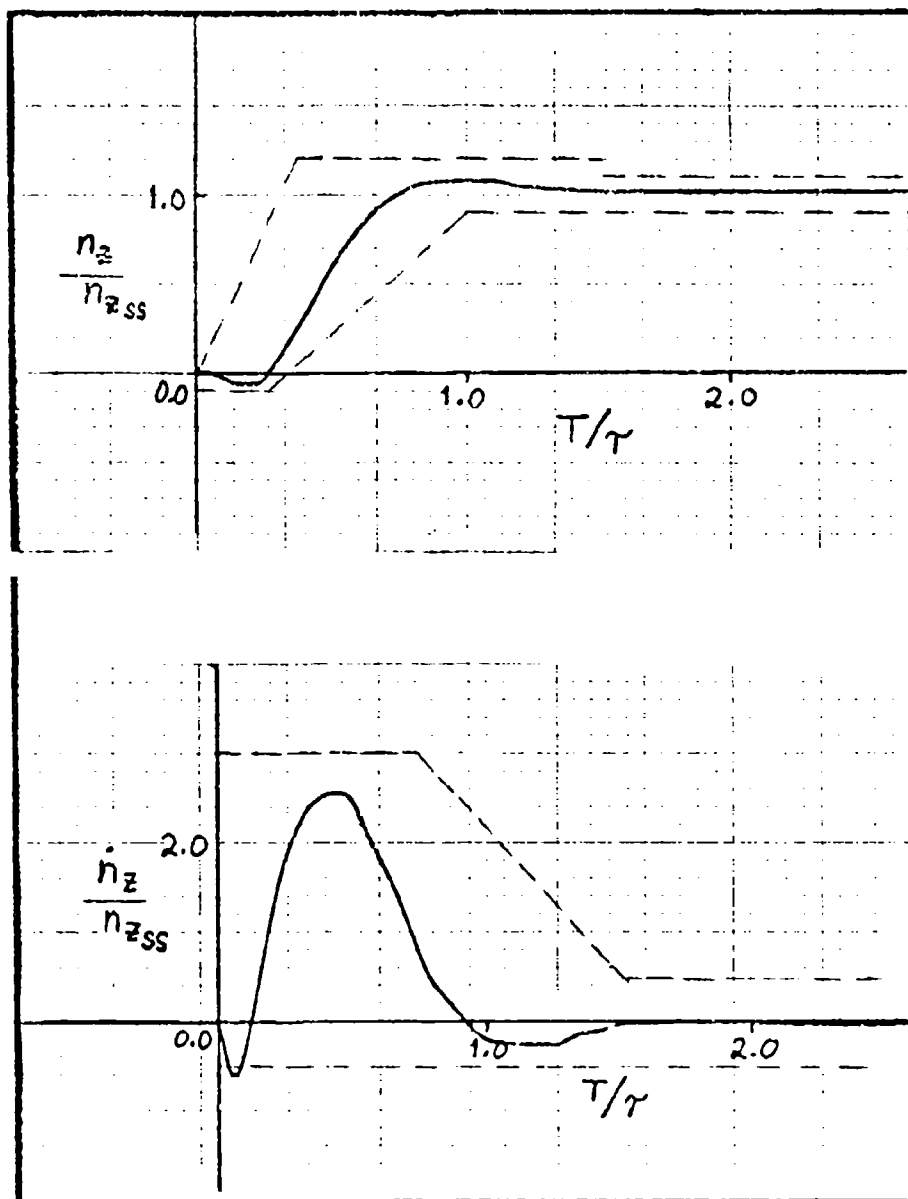


Figure 23. Closed-loop aircraft response with Pre-Filter for Flight Condition 3; Break Frequency 1 rad/sec.

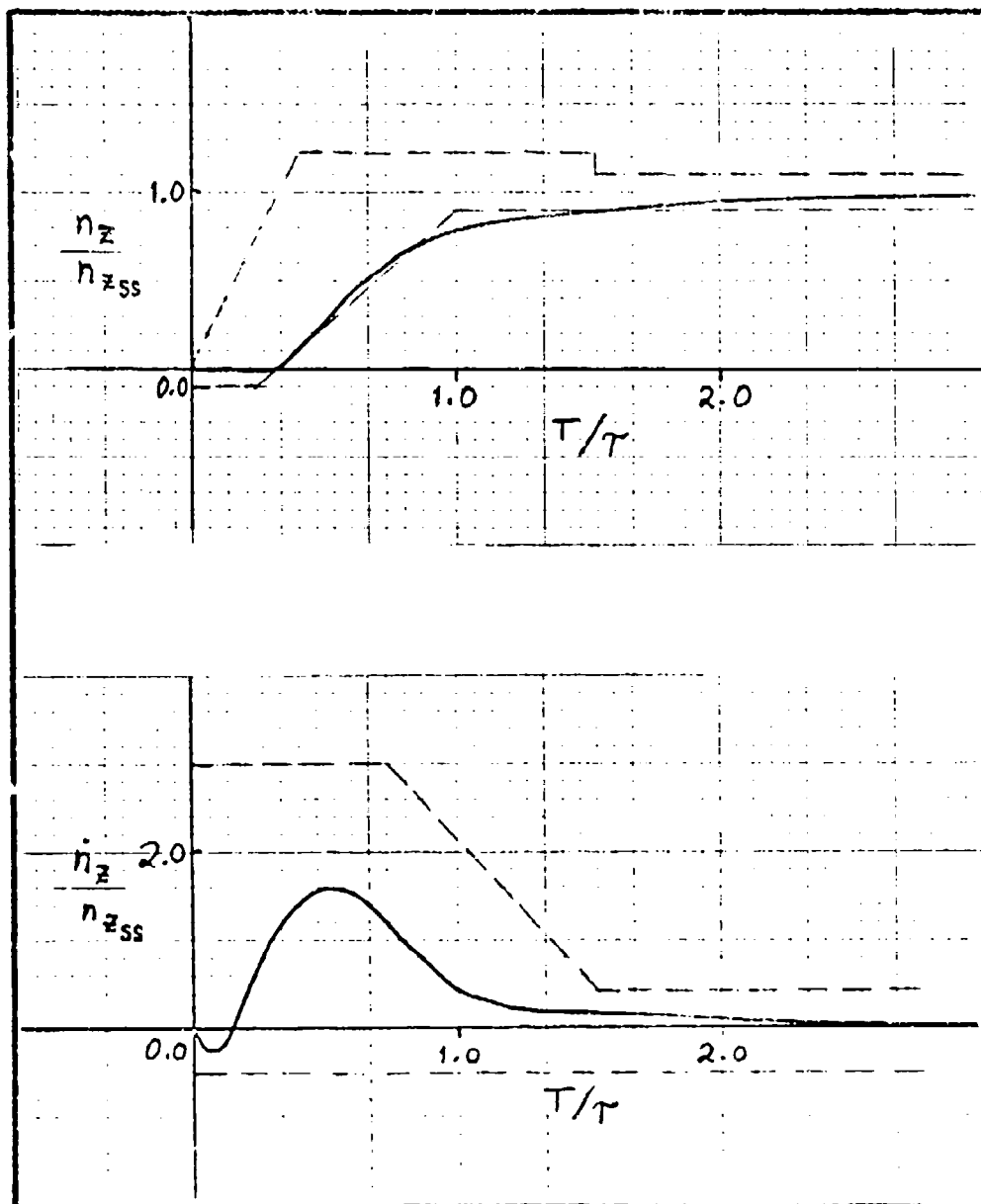


Figure 21. Model I, of Aircraft Response with Pre-filter for Pilot Control 2; Peak Frequency, 2 rad/sec.

GGC/EE/73-3

Flight Condition 5

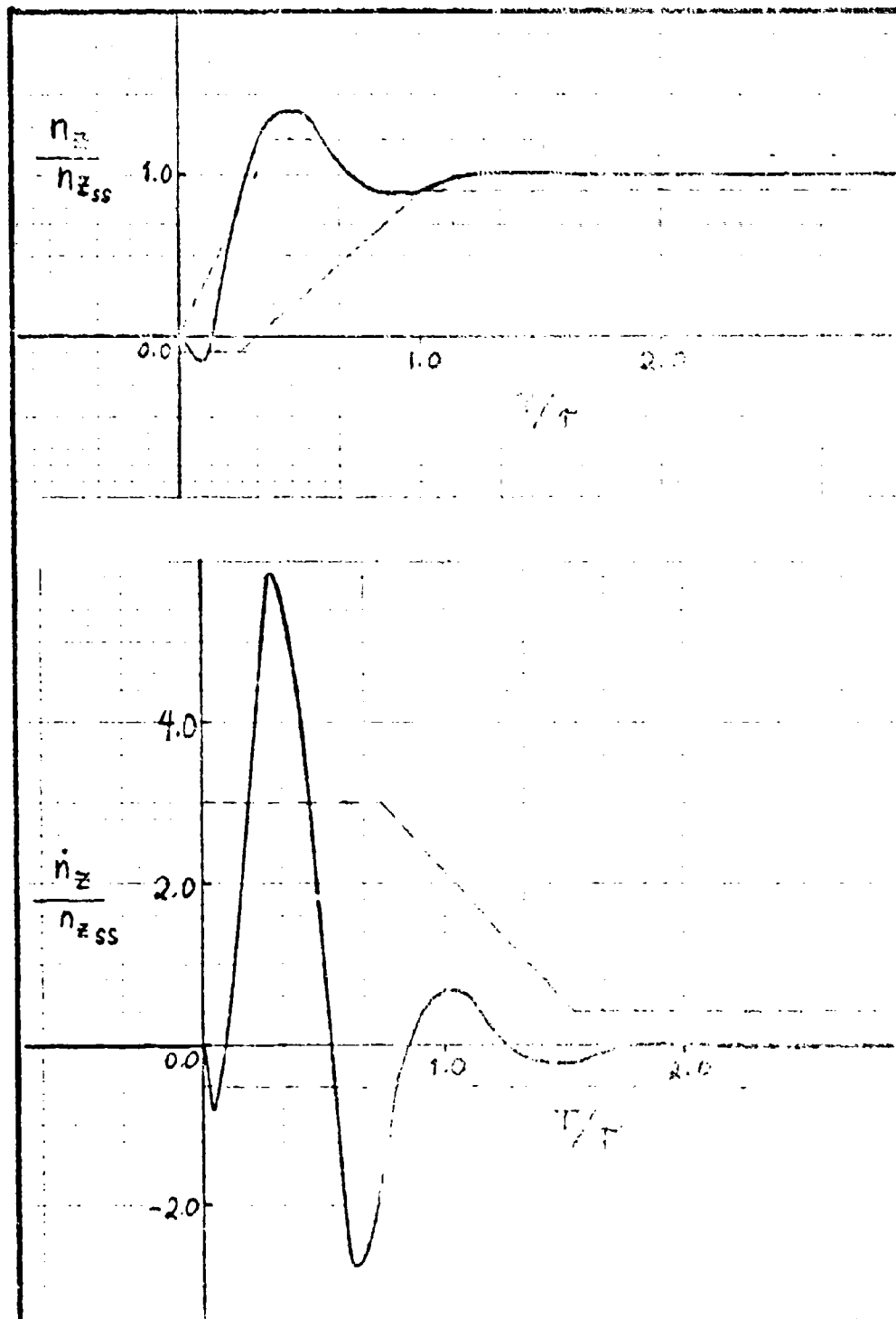
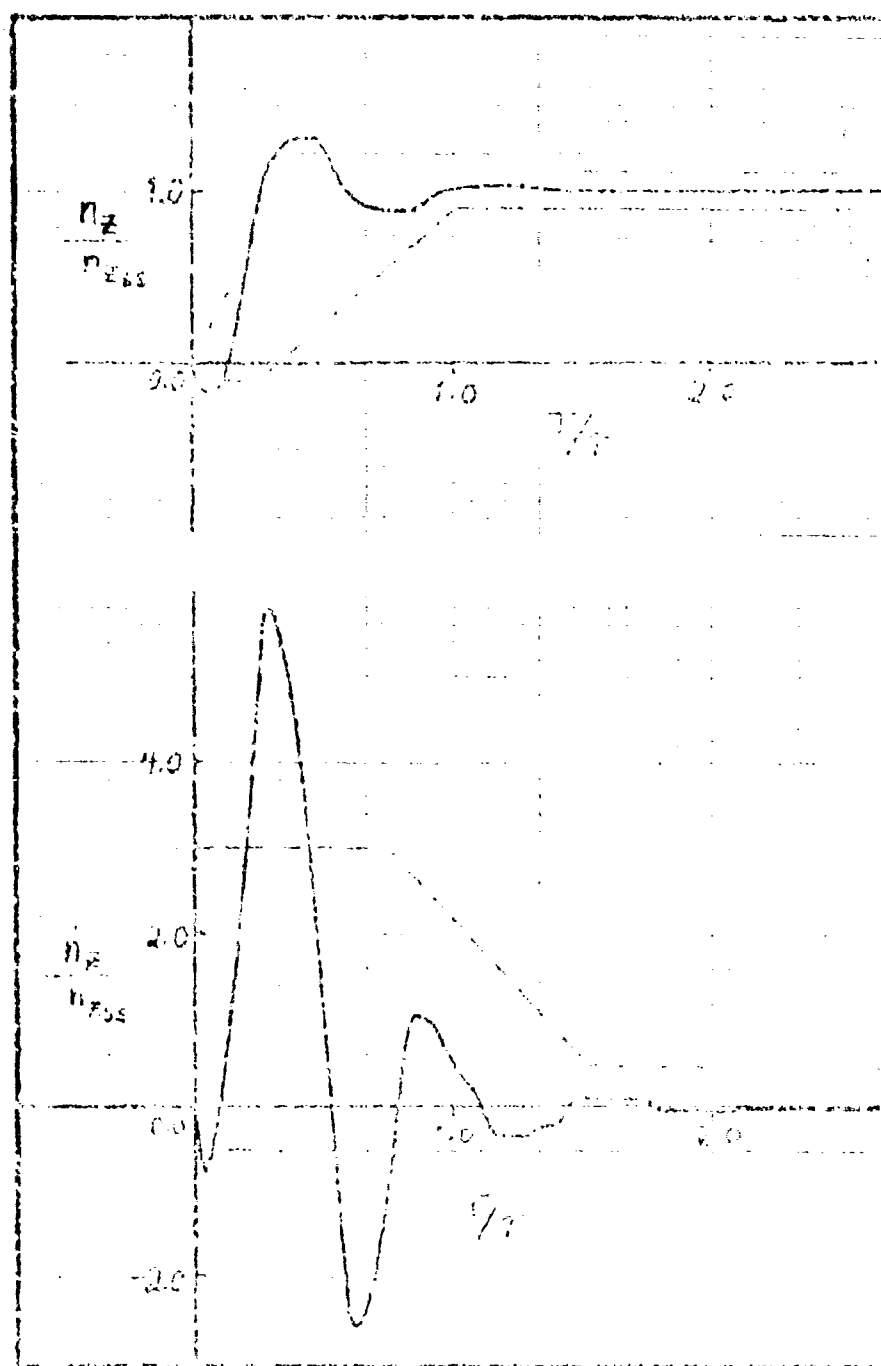


Figure 22. (a) $\frac{n_z}{n_{zss}}$ vs. T/τ
 Condition: \dots

GSC/ES/75-5



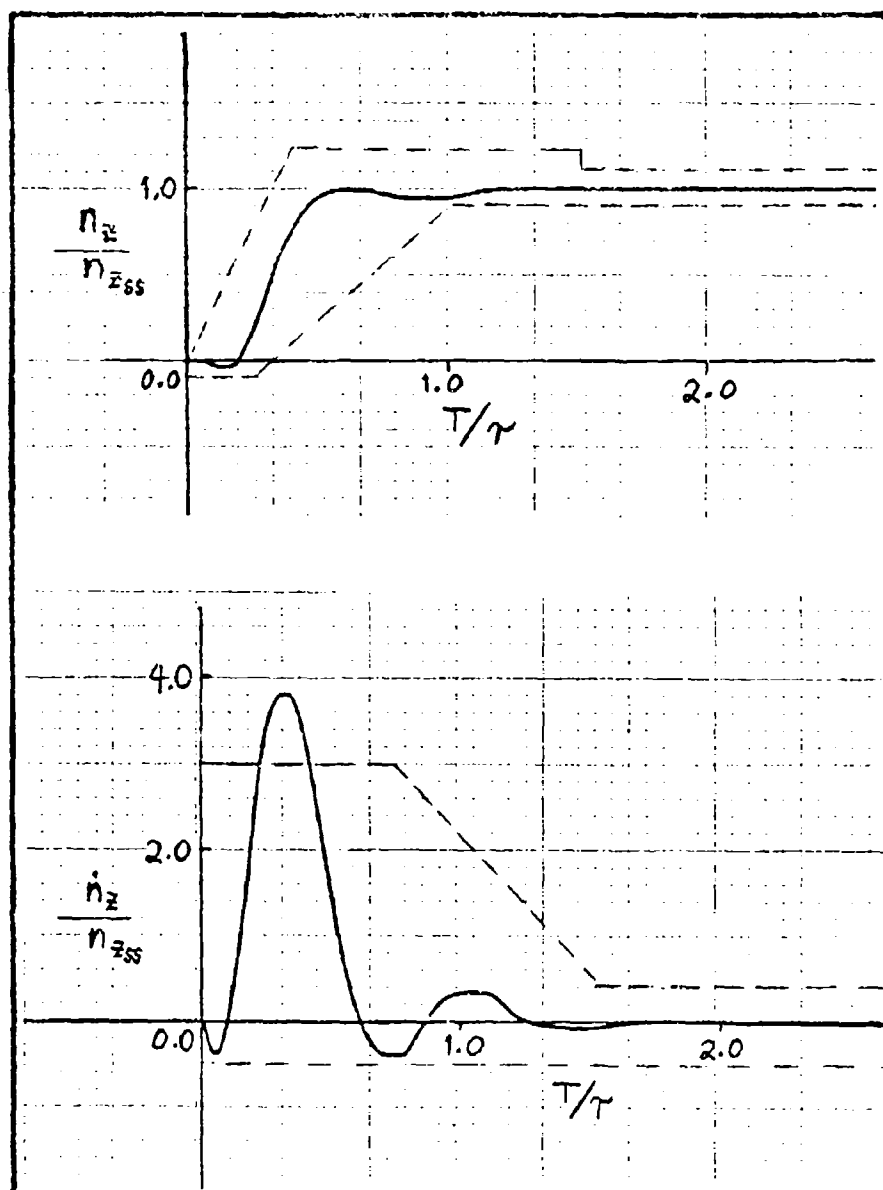


Figure 24. Closed Loop Aircraft Response with Pre-Filter for Flight Condition 5; Break Frequency 5 rad/sec.

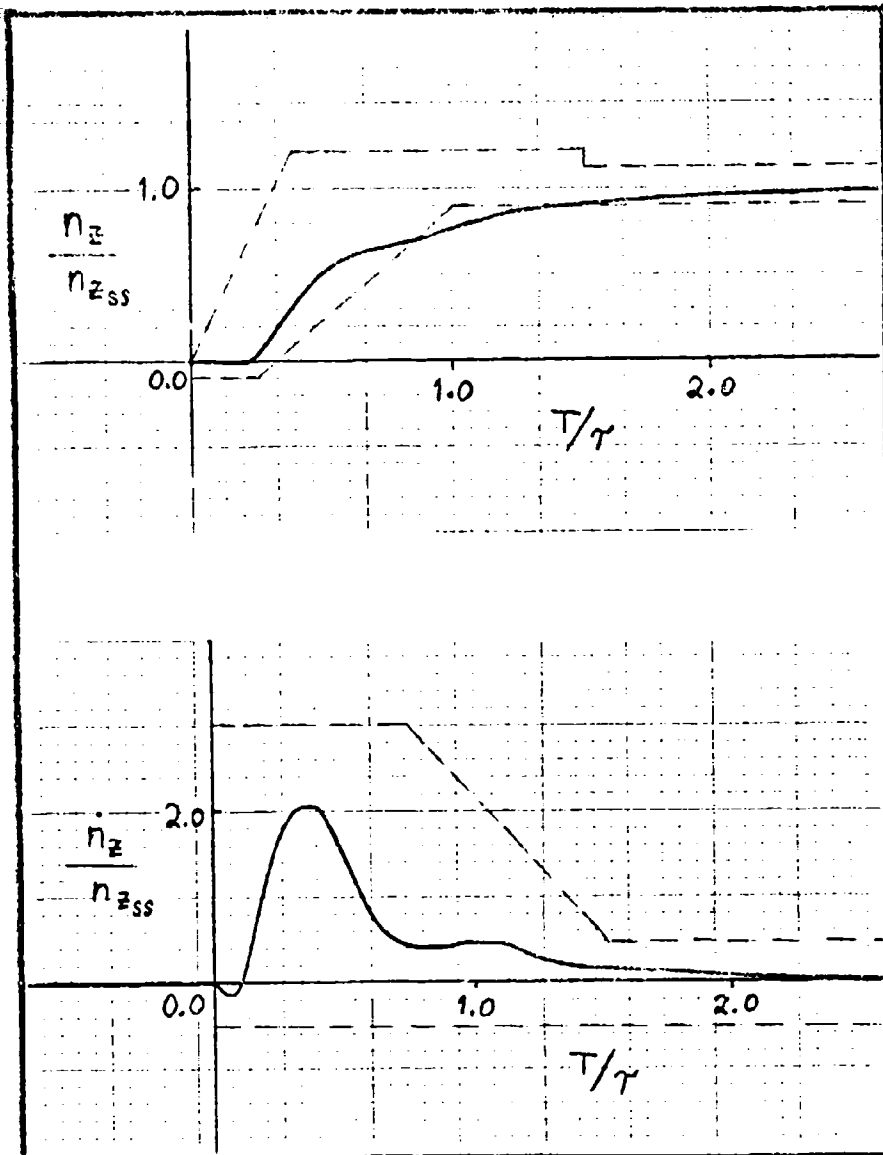


Figure 25. Closed Loop Aircraft Response with Pre-Filter for Flight Condition 5; Frequency 2 rad/sec.

GGC/EE/73-3

Flight Condition 9

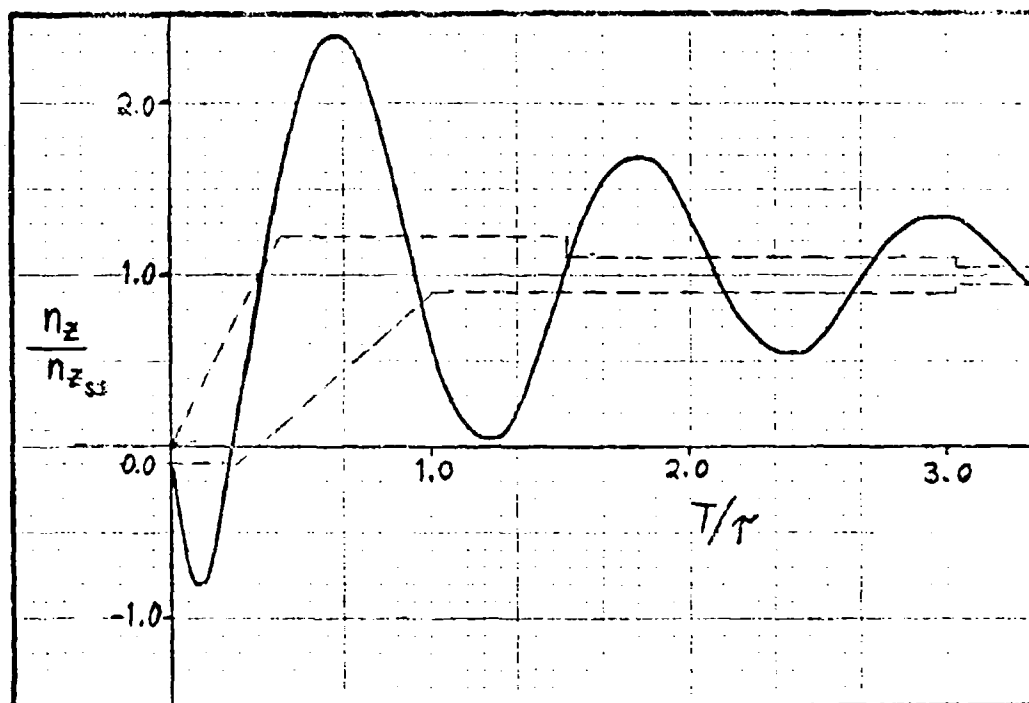


Figure 26. Open Loop Aircraft n_z Response for Flight Condition 9.

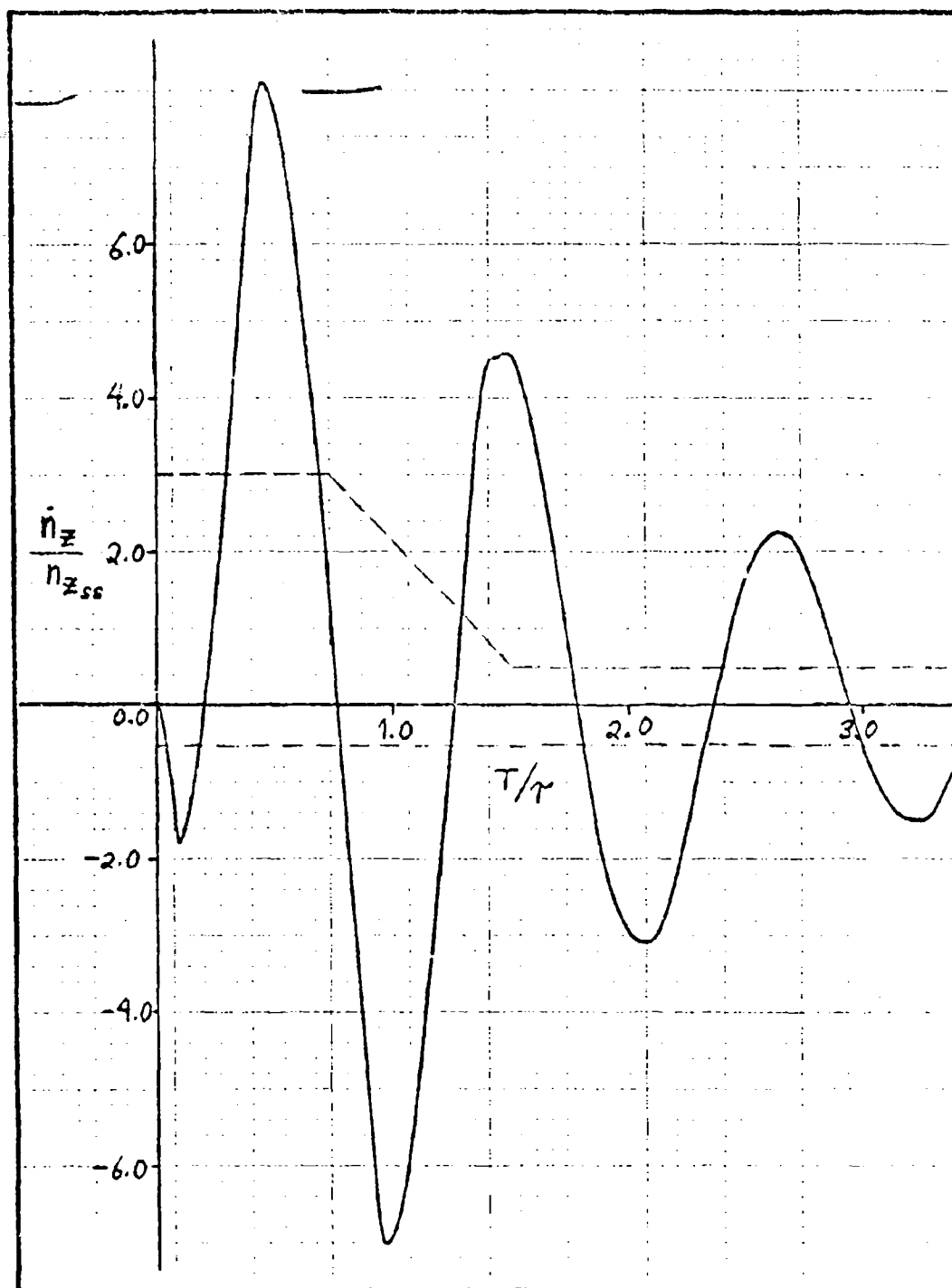


Figure 27. Open Loop Aircraft \dot{A}_z Response for Flight Condition 9.

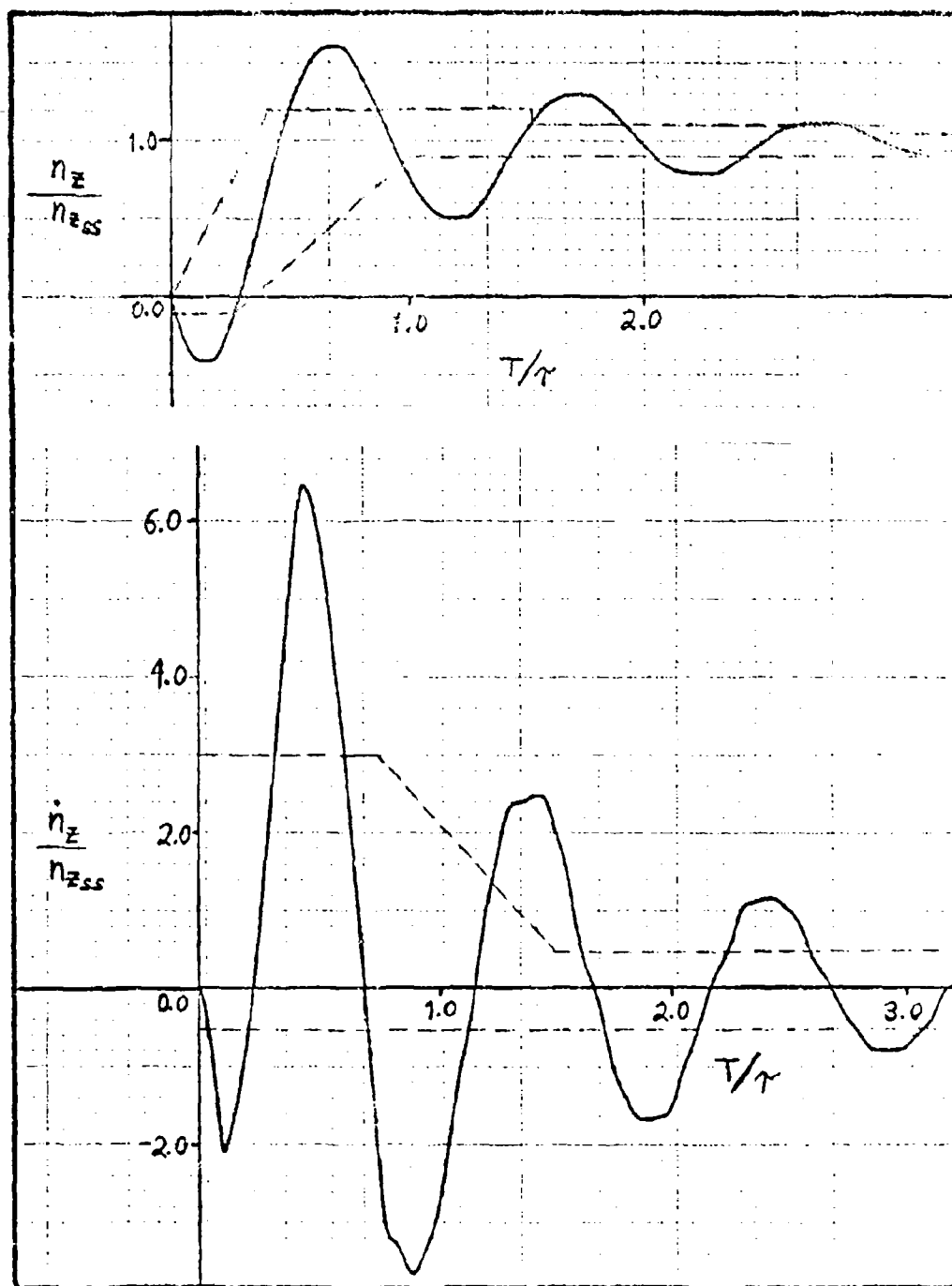


Figure 28. Closed loop aircraft response for Flight Condition 2.

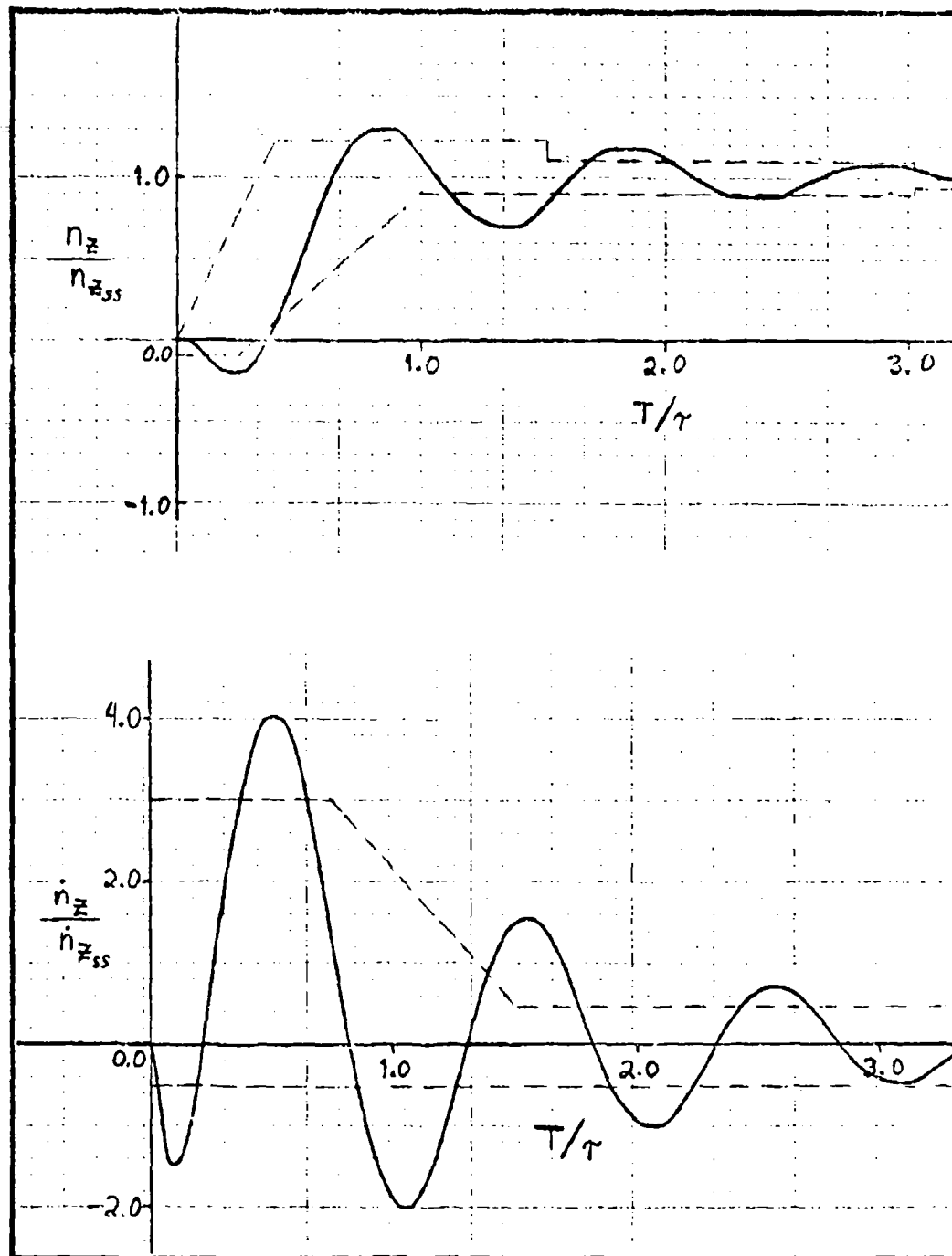


Figure 29. Closed Loop Aircraft Response with Pre-Filter for Flight Condition 9; Break Frequency 5 rad/sec.

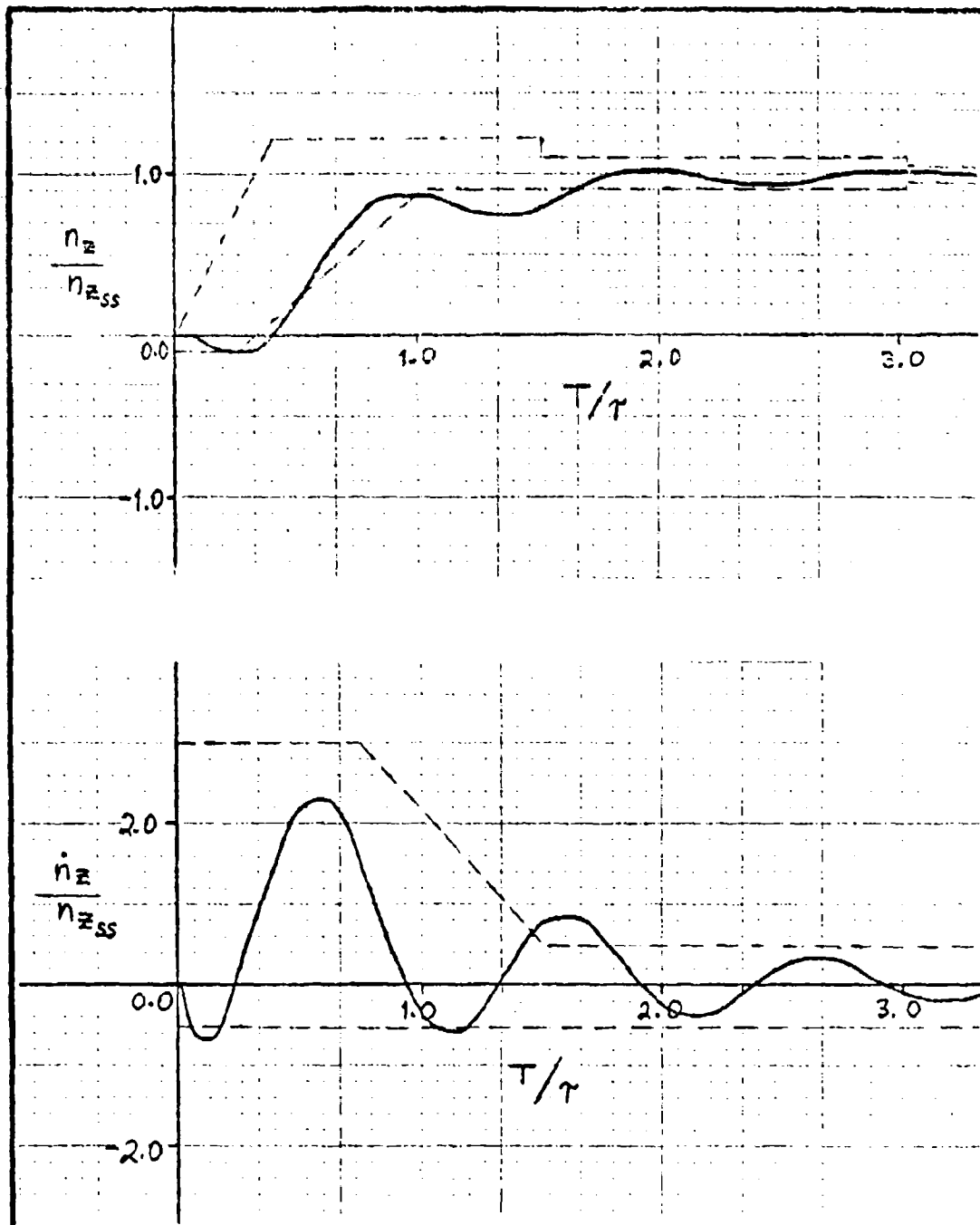


Figure 30. Closed Loop Aircraft Response with Pre-Filter for Flight Condition 9; Break Frequency 2 rad/sec.



GSC/22/73-3

Flight Condition 13

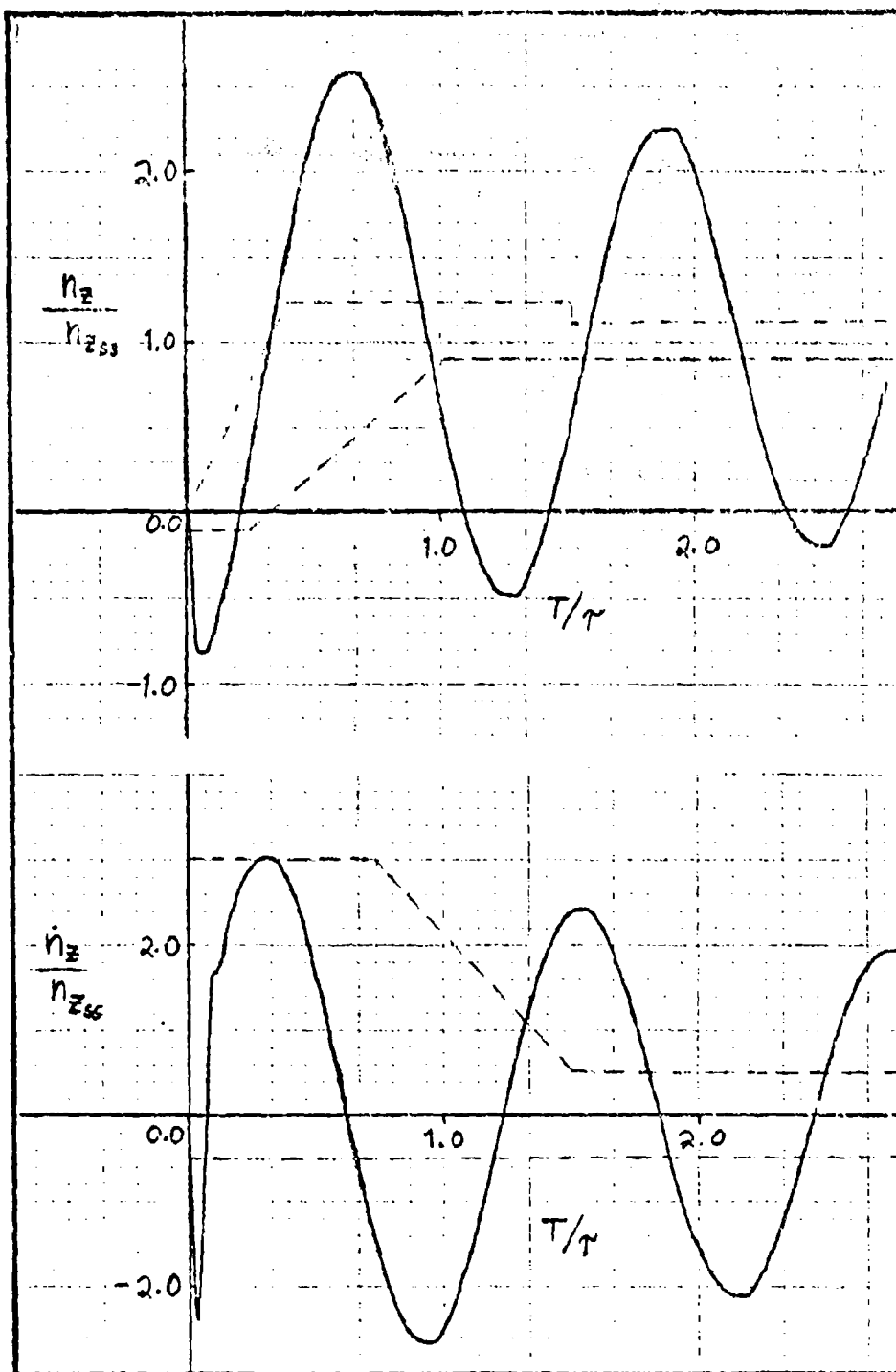


Figure 31. Open Loop Aircraft Response for Flight Condition 15.

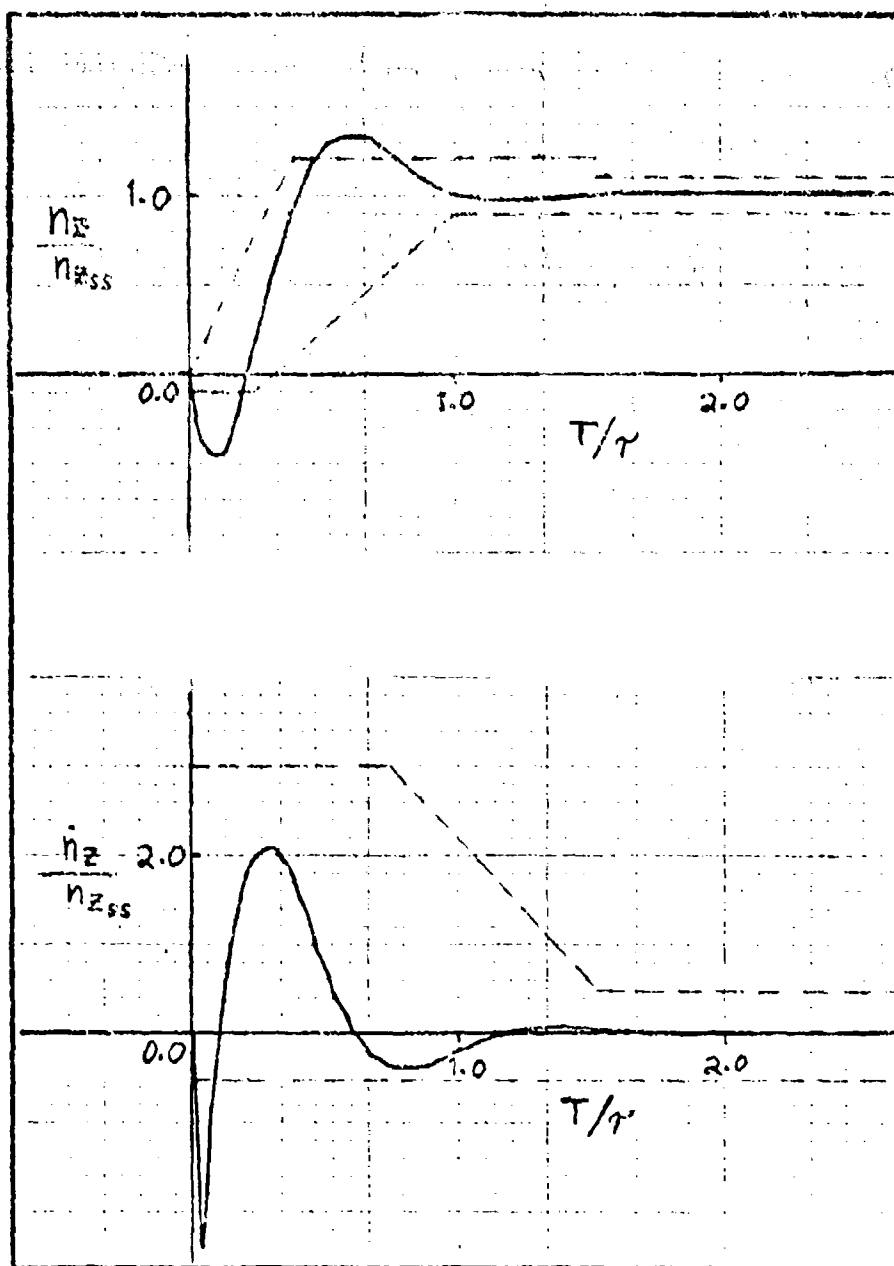


Figure 32. Closed loop Aircraft response for Flight Condition 13.

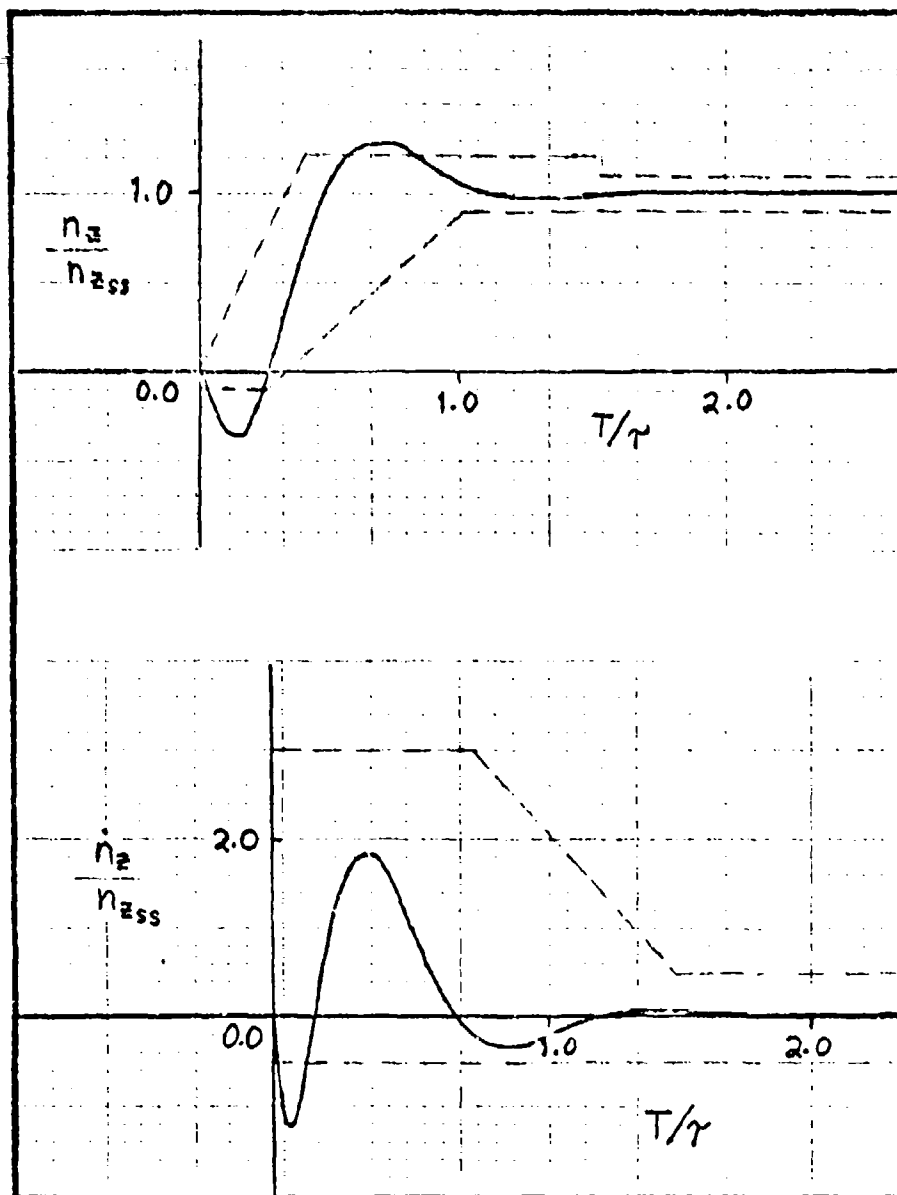


Figure 33. Closed Loop Aircraft Response with Pre-Filter for Flight Condition 13; Break Frequency 5 rad/sec.

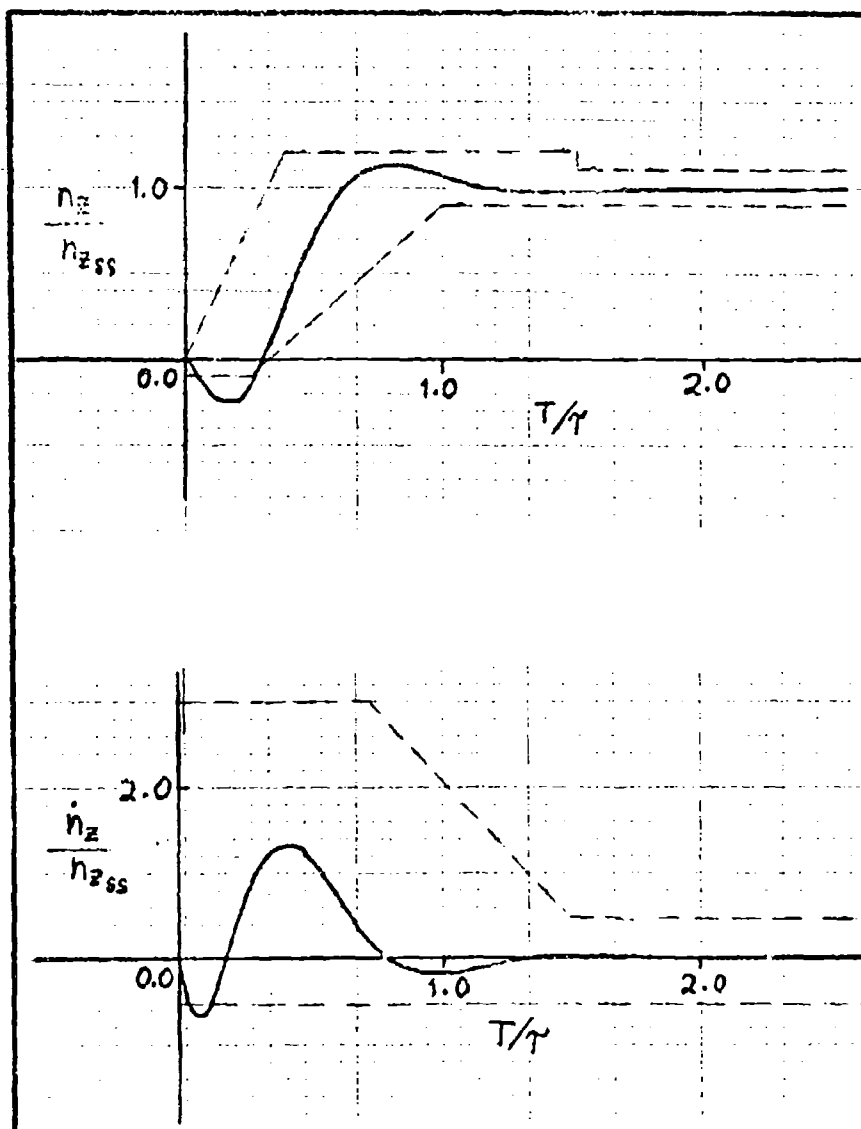


Figure 34. Closed Loop Aircraft Response with Pre-Filter for Flight Condition 13; Break Frequency 2 rad/sec.



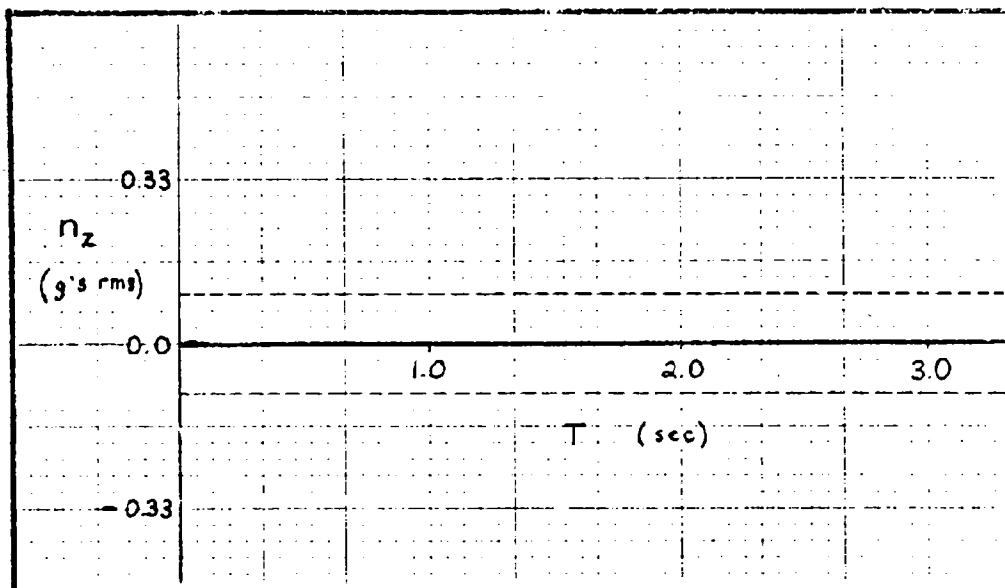


Figure 35. Typical Aircraft Response to a Specified Vertical Wind Gust.

Appendix D

Pre-Filter Equations

From Figure 12

$$\delta_p = \delta + \delta_r \quad (66)$$

$$\delta_e = \delta_p' - \delta_s \quad (67)$$

$$\omega_p \delta_p = \dot{\delta}_p' + \omega_p \delta_p' \quad (68)$$

From Appendix B,

$$\delta = y_1 - \frac{1}{T_I} y_2 - \frac{K_p T_L}{T_I} \theta_c \quad (69)$$

Substituting equation (69) into equation (66), and then into equation (68)

$$\begin{aligned} \omega_p y_1 - \frac{\omega_p}{T_I} y_2 - \frac{\omega_p K_p T_L}{T_I} \theta_c + \omega_p \delta_r \\ = \dot{\delta}_p' + \omega_p \delta_p' \end{aligned} \quad (70)$$

The resulting new state equation for δ_p' is

$$\dot{\delta}_p' = \omega_p y_1 - \frac{\omega_p}{T_I} y - \frac{\omega_p K_p T_L}{T_I} \theta_c + \omega_p \delta_r - \omega_p \delta_p' \quad (71)$$

Also from Figure 12

$$\dot{\delta}_e = \frac{1}{T_e} \delta_r - \frac{1}{T_e} \delta_e \quad (72)$$

Substituting equation (67) into equation (72) yields

$$\dot{\delta}_e = \frac{1}{T_e} \delta_p' - \frac{1}{T_e} \delta_s - \frac{1}{T_e} \delta_e \quad (73)$$

Since from Appendix A

$$\dot{\delta}_s = K_s \delta_e + \beta \quad (59)$$

Preceding page blank

we can substitute equation (59) into equation (73) to get the state equation in δ_e .

$$\dot{\delta}_e = \left[-\frac{1}{T_e}(1+\kappa_f) \right] \delta_e - \frac{1}{T_e} \beta + \frac{1}{T_e} \delta_p' \quad (74)$$

which is a change to the previous equation for δ_e .

Vita

Robert Peter Denaro was born on 28 January 1949 in Glen Rock, New Jersey. He moved to Valhalla, New York in 1954, and graduated from Valhalla High School in 1967. He graduated from the United States Air Force Academy in June 1971 with a Bachelor of Science Degree in Engineering Sciences with a major in Astronautics. Commissioned an Air Force Second Lieutenant upon graduation, he entered the Air Force Institute of Technology to pursue a Master of Science Degree in Electrical Engineering in the Graduate Guidance and Control Curriculum.

Permanent address: 2871 College Hill Ct.
Fairborn, Ohio
45324

Vita

Garrison Lee Greenleaf was born on 2 March 1943 in Snohomish, Washington. He graduated from Snohomish High School in 1967. He graduated from the United States Air Force Academy in June 1971 with a Bachelor of Science Degree in Engineering Sciences and a commission as an Air Force Second Lieutenant. His first and only assignment was to the Air Force Institute of Technology to pursue a Master of Science Degree in Electrical Engineering in the Guidance and Control Curriculum.

Permanent address: Route 1, Box 186
Snohomish, Washington
98290